

**Lect. 2. Holographic Transforms in Digital Computers****2.1. Mathematical models of recording and reconstruction of holograms**

Consider schematic diagram of recording hologram shown in Fig. 1. In hologram recording, an object whose hologram is to be recorded is illuminated by a coherent radiation from a radiation source, which simultaneously illuminates also a hologram-recording medium with a “reference” beam. Usually, the photosensitive surface of the recording medium is a plane. We refer to this plane as a hologram plane. At each point of the hologram plane, the recording medium, whether it is continuous, such as a photographic film, or discrete, such as a photosensitive array of CMOS or CCD digital cameras, measures energy of the sum of the reference beam and the object beam reflected or transmitted by the object.

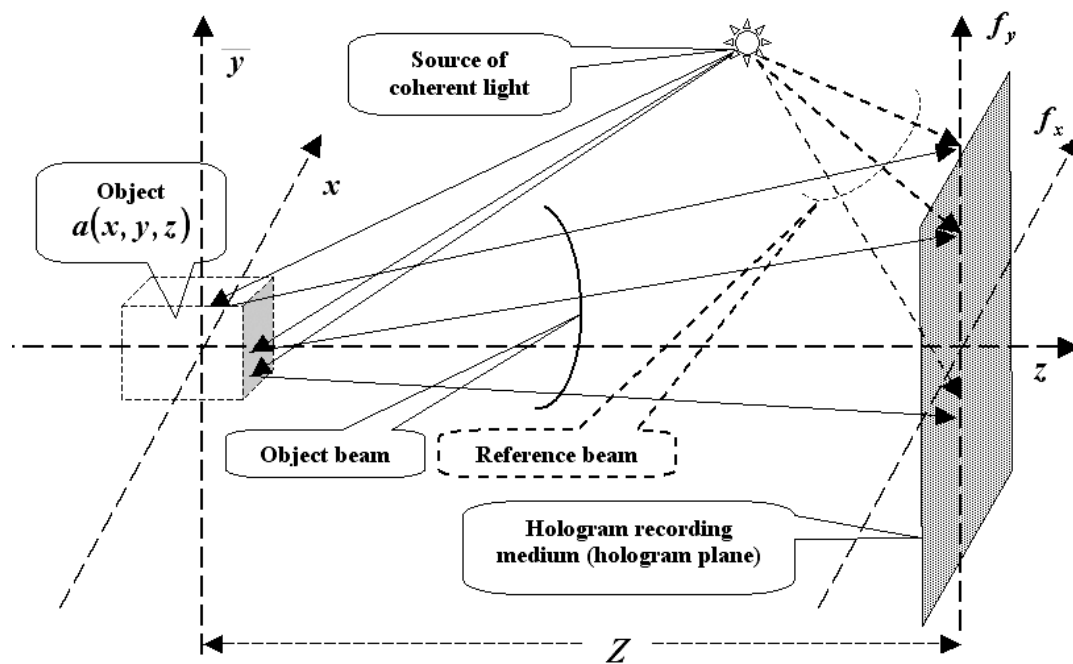


Fig. 1. Schematic diagram of hologram recording

Conventional mathematical models of recording and reconstruction of holograms assume that: (i) monochromatic coherent radiation that can be described by its complex amplitude as a function of spatial coordinates is used for hologram recording and reconstruction and (ii) object characteristics defining its ability to reflect or transmit incident radiation are described by radiation reflection or transmission factors which are also functions of spatial coordinates. Specifically, if  $I(x, y, z)$  is complex amplitude of the object illumination radiation at point  $(x, y, z)$ , complex amplitude  $a(x, y, z)$  of the radiation reflected or transmitted by the object at this point is defined by the equation:

$$a(x, y, z) = I(x, y, z)O(x, y, z) \quad (2.1.1)$$

where  $O(x, y, z)$  is object reflection or, correspondingly, transmission factor.

If  $\alpha(f_x, f_y)$  and  $R(f_x, f_y)$  denote complex amplitudes of the object and reference beams, respectively, at point  $(f_x, f_y)$  of the hologram plane, signal recorded by the recording medium at this point is a squared module of their sum:

$$\begin{aligned} H(f_x, f_y) &= |\alpha(f_x, f_y) + R(f_x, f_y)|^2 = \\ &= \alpha(f_x, f_y)R^*(f_x, f_y) + \alpha^*(f_x, f_y)R(f_x, f_y) + |\alpha(f_x, f_y)|^2 + |R(f_x, f_y)|^2, \end{aligned} \quad (2.1.2)$$

where asterisk denotes complex conjugate. This signal is a hologram signal, or a hologram. The first term in the sum in the right hand part of Eq. 2.1.2 is proportional to the object's beam complex amplitude. We will call this term a “*mathematical hologram*”. Hologram reconstruction consists in applying to the mathematical hologram a transform that implements wave back propagation from the hologram plane to object. For this, one has either to eliminate, before the reconstruction, other three terms or to apply the reconstruction transform to the entire hologram and then separate the contribution of other terms in the reconstruction result from that of the mathematical hologram term.

As it is known, wave propagation transformations are, from the signal theory point of view, linear transformations. As such, they are mathematically modeled as integral transformation. Thus, object complex amplitude of radiation  $a(x, y, z)$  and object beam wave front  $\alpha(f_x, f_y)$  at hologram plane are related through “forward propagation”

$$\alpha(f_x, f_y) = \int_{-\infty}^{\infty} \int_{-\infty}^{\infty} \int_{-\infty}^{\infty} a(x, y, z) WPK(x, y, z; f_x, f_y) dx dy dz \quad (2.1.3, a)$$

and “backward propagation”

$$a(x, y, z) = \int_{-\infty}^{\infty} \int_{-\infty}^{\infty} \alpha(f_x, f_y) WPK(x, y, -z; f_x, f_y) df_x df_y \quad (2.1.3, b)$$

integral transforms, where  $WPK(.,.)$  is a transform (wave propagation) kernel. Commonly, this model is simplified by considering wave propagation between plane slices of the object and the hologram plane:

$$\alpha(f_x, f_y) = \int_{-\infty}^{\infty} \int_{-\infty}^{\infty} a(x, y, 0) WPK(x, y, Z; f_x, f_y) dx dy \quad (2.1.4, a)$$

and

$$a(x, y, 0) = \int_{-\infty}^{\infty} \int_{-\infty}^{\infty} \alpha(f_x, f_y) WPK(x, y, -Z; f_x, f_y) df_x df_y, \quad (2.1.4, b)$$

where  $Z$  is the distance between the object and hologram planes. Equations (2.1.4) are called diffraction transforms.

## 2.2. Diffraction integrals

Diffraction transforms of Eqs. 2.1.3 and 2.1.4 are treated in digital holography with the help of the scalar diffraction theory of light propagation. According to the theory, wave front  $\alpha(\mathbf{f})$  of an object  $a(\mathbf{x})$  is defined by the Kirchhoff-Rayleigh-Sommerfeld integral ([1]):

$$\alpha(\mathbf{f}) = \int_{-\infty}^{\infty} a(\mathbf{x}) \frac{Z}{R} \left( 1 - i \frac{2\pi}{\lambda} R \right) \frac{\exp(i2\pi R/\lambda)}{R^2} d\mathbf{x}, \quad (2.2.1)$$

where  $\mathbf{x} = (x, y)$  is a coordinate vector in the object plane,  $\mathbf{f} = (f_x, f_y)$  is a coordinate vector in the hologram plane,  $Z$  is a distance between object and hologram planes,  $R = \sqrt{Z^2 + \|\mathbf{x} - \mathbf{f}\|^2}$ ,  $\|\cdot\|$  symbolizes vector norm and  $\lambda$  is the radiation wavelength.

Usually, an approximation to the integral (2.2.1) is made:

$$\left( 1 - i \frac{2\pi}{\lambda} R \right) \approx i \frac{2\pi}{\lambda} R, \quad (2.2.2)$$

and the above integral is reduced to

$$\alpha(f) \approx -i \frac{2\pi}{\lambda} Z \int_{-\infty}^{\infty} a(x) \frac{\exp(i2\pi R/\lambda)}{R^2} dx \propto \int_{-\infty}^{\infty} a(x) \frac{\exp\left( i2\pi \frac{Z\sqrt{1+(x-f)^2/Z^2}}{\lambda} \right)}{1+(x-f)^2/Z^2} dx. \quad (2.2.3)$$

We call this transform *Kirchhoff-Rayleigh-Sommerfeld integral transform (KRST)*. This relationship is illustrated in Fig. 2.1.

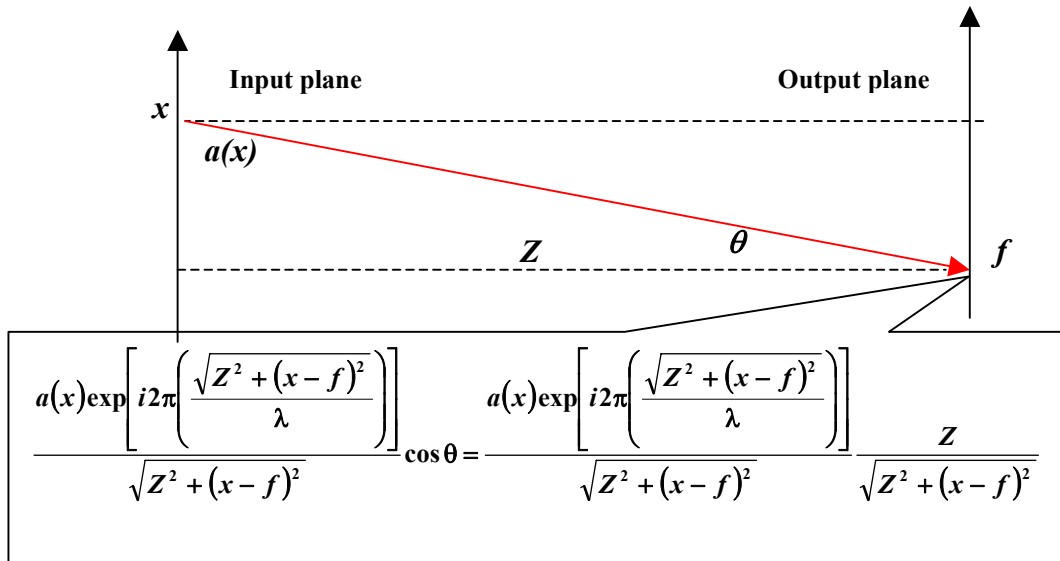


Fig. 2.1. Graphical illustration of the wave propagation model

In what follows, we, for the sake of brevity, will use one-dimensional denotation unless otherwise is indicated.

Most frequently, object size and hologram size are small with respect to the object-to-hologram distance  $Z$ . Depending on how small they are, two other approximations to the Kirchhoff - Rayleigh-Sommerfeld integral (Eq. 2.2.3) are used, “near zone diffraction” (Fresnel) approximation:

$$\alpha(f) \propto \int_{-\infty}^{\infty} a(x) \exp\left[i\pi \frac{(x-f)^2}{\lambda Z}\right] dx \quad (2.2.4)$$

known as *Fresnel integral transform*, and “far zone diffraction” (Fraunhofer) approximation which is well known *Fourier integral transform*.

$$\alpha(f) \propto \int_{-\infty}^{\infty} a(x) \exp\left(-i2\pi \frac{xf}{\lambda Z}\right) dx \quad (2.2.5)$$

There is also a version of the Fresnel Transform called *angular spectrum propagation* ([1]). In this version, Fresnel Transform is treated as a convolution.

By the Fourier convolution theorem, Fresnel transform (Eq. 2.2.4) can be represented as inverse Fourier Transform

$$\begin{aligned} \alpha(f) \propto \int_{-\infty}^{\infty} \left[ \int_{-\infty}^{\infty} a(x) \exp(i2\pi x\xi) dx \right] \left[ \int_{-\infty}^{\infty} \exp\left(i\pi \frac{x^2}{\lambda Z}\right) \exp(i2\pi x\xi) dx \right] \exp(-i2\pi f\xi) d\xi \propto \\ \int_{-\infty}^{\infty} \left[ \int_{-\infty}^{\infty} a(x) \exp(i2\pi x\xi) dx \right] \exp(-i\pi \lambda Z \xi^2) \exp(-i2\pi f\xi) d\xi \end{aligned} \quad (2.2.6)$$

of the product of signal Fourier Transform and Fourier Transform of the chirp function  $\exp(i\pi x^2/\lambda Z)$ , which is, in its turn, a chirp-function (Appendix A.2.2, Eq. A.2.2.1).

For numerical reconstruction of holograms recorded in different diffraction zones, as well as for synthesis of computer generated holograms, discrete representations of the above diffraction integrals are needed that are suited for efficient computational implementation.

### 2.3. Discrete representation of transforms: principles

As far as quantum effects are not concerned, physical reality is a continuum whereas computers have only finite number of discrete states. How can one imitate physical reality of optical signals and transforms in computers? Two principles lie in the base of digital representation of continuous signal transformations: the *conformity principle* with digital representation of signals and the *mutual correspondence principle* between continuous and discrete transformations ([2]). The conformity principle requires that digital representation of signal transformations should parallel that of signals. Mutual correspondence between continuous and digital transformations is said to hold if both act to transform identical input signals into identical output signals. According to these principles, digital processors incorporated into optical information systems should be regarded and treated together with signal digitization and signal reconstruction devices as integrated analogous units.

Discretization is a process of measuring, in the discretization devices such as image scanners and hologram sensors, of coefficients of signal expansion into a series over a set of functions called **discretization basis functions**. These coefficients represent signals in computers. It is assumed that original continuous signals can be, with certain agreed accuracy, reconstructed by summation of functions called **reconstruction basis functions** with weights equal to the corresponding coefficients of signal discrete representation. The reconstruction is carried out in signal reconstruction devices such as, for instance, image displays and computer generated hologram recorders.

In digital holography and digital image processing, discretization and reconstruction basis functions that belong to a family of “**shift**”, or sampling, **basis functions** are most commonly used. All functions from this family are obtained from one “mother” function by means of its spatial shifts through multiple of a **sampling interval**. Signal discrete representation coefficients obtained for such functions are called **signal samples**.

The mathematical formulation of signal sampling and reconstruction from the sampled representation is as follows. Let  $\mathbf{a}(\mathbf{x})$  be a continuous signal as a function of spatial co-ordinates given by a vector  $\mathbf{x}^{(s)}$ ,

$$\varphi_k^{(s)}(\mathbf{x}^{(s)}) = \varphi^{(s)}(\mathbf{x}^{(s)} - \tilde{\mathbf{k}}^{(s)} \Delta \mathbf{x}^{(s)}) \quad \text{and} \quad \varphi_k^{(r)}(\mathbf{x}^{(r)}) = \varphi^{(r)}(\mathbf{x}^{(r)} - \tilde{\mathbf{k}}^{(r)} \Delta \mathbf{x}^{(r)}) \quad (2.3.1)$$

be sampling and reconstruction basis functions defined in the sampling and reconstruction devices coordinates  $\{\mathbf{x}^{(s)}\}$  and  $\{\mathbf{x}^{(r)}\}$ , respectively,  $\Delta \mathbf{x}^{(s)}$  and  $\Delta \mathbf{x}^{(r)}$  be vectors of the sampling intervals in, respectively, sampling and reconstruction devices,  $\tilde{\mathbf{k}}^{(s)} = \mathbf{k} + \mathbf{u}^{(s)}$  and  $\tilde{\mathbf{k}}^{(r)} = \mathbf{k} + \mathbf{u}^{(r)}$  be vectors of signal sample indices  $\mathbf{k}$  biased by certain shift vectors  $\mathbf{u}^{(s)}$  and  $\mathbf{u}^{(r)}$ . Shift vectors describe shift, in units of the corresponding sampling intervals, of the sampling grid with respect to the corresponding coordinate systems  $\mathbf{x}^{(s)}$  and  $\mathbf{x}^{(r)}$  such that samples with index  $\mathbf{k} = \mathbf{0}$  are assumed to have respective coordinates  $\mathbf{x}^{(s)} = \mathbf{u}^{(s)}$ ,  $\mathbf{x}^{(r)} = \mathbf{u}^{(r)}$

At sampling, signal samples  $\{a_k\}$  are computed as projections of the signal onto sampling basis functions:

$$a_k = \int_{\mathbf{x}} \mathbf{a}(\mathbf{x}) \varphi^{(s)}(\mathbf{x}^{(s)} - \tilde{\mathbf{k}}^{(s)} \Delta \mathbf{x}^{(s)}) d\mathbf{x}, \quad (2.3.2)$$

assuming certain relationship between signal and sampling device coordinate systems  $\{\mathbf{x}\}$  and  $\{\mathbf{x}^{(s)}\}$ .

Signal reconstruction from the set of their samples  $\{a_k\}$  is described as signal expansion over the set of reconstruction basis functions:

$$\tilde{\mathbf{a}}(\mathbf{x}^{(r)}) = \sum_{\mathbf{k}} a_{\mathbf{k}} \varphi^{(r)}(\mathbf{x}^{(r)} - \tilde{\mathbf{k}}^{(r)} \Delta \mathbf{x}^{(r)}) \quad (2.3.3)$$

in a reconstruction device coordinate system.

The result  $\tilde{\mathbf{a}}(\mathbf{x})$  of the signal reconstruction from its discrete representation obtained according to Eq. 2.3.3 is not, in general, identical to the initial signal  $\mathbf{a}(\mathbf{x})$ . It

is understood, however, that it can, in the given application, serve as a substitute for the initial signal.

Eqs. 2.3.2 and 2.3.3 model processes of hologram sampling in digital cameras and, respectively, object reconstruction in display devices.

According to the above-formulated conformity principle, Eqs. 2.3.2 and 2.3.3 form the base for adequate discrete representation of signal transformations. In what follows, we describe discrete representations of optical diffraction integral transforms generated by this kind of signal representation.

## 2.4. Discrete Fourier transforms

In this section, we will provide, using the above outlined approach, a full derivation of discrete Fourier transforms as discrete representations of the integral Fourier Transform. This derivation will explicitly demonstrate approximations that are done in this continuous-to-discrete conversion and will serve as an illustrative model for other diffraction transforms considered hereafter.

Let  $\alpha(f)$  and  $a(x)$  be, correspondingly, hologram and object wave fronts linked through the integral Fourier Transform:

$$\alpha(f) = \int_{-\infty}^{\infty} a(x) \exp\left(i2\pi \frac{xf}{\lambda Z}\right) dx \quad (2.4.1)$$

In digital recording of holograms, samples of the hologram wave front are obtained as

$$\alpha_r = \int_{-\infty}^{\infty} \alpha(f) \varphi^{(s)}(f - \tilde{r}^{(s)} \Delta f^{(s)}) df \quad (2.4.2)$$

Replacing here  $\alpha(f)$  through its representation as Fourier transform of  $a(x)$  (Eq. 2.4.1), we obtain:

$$\begin{aligned} \alpha_r &= \int_{-\infty}^{\infty} \left\{ \int_{-\infty}^{\infty} a(x) \exp\left(i2\pi \frac{xf}{\lambda Z}\right) dx \right\} \varphi^{(s)}(f - \tilde{r}^{(s)} \Delta f^{(s)}) df = \\ &= \int_{-\infty}^{\infty} a(x) dx \left\{ \int_{-\infty}^{\infty} \varphi^{(s)}[f - \tilde{r}^{(s)} \Delta f^{(s)}] \exp\left(i2\pi \frac{xf}{\lambda Z}\right) df \right\} = \\ &= \int_{-\infty}^{\infty} a(x) \exp\left(i2\pi \frac{x\tilde{r}^{(s)} \Delta f^{(s)}}{\lambda Z}\right) dx \left\{ \int_{-\infty}^{\infty} \varphi^{(s)}(f) \exp\left(i2\pi \frac{xf}{\lambda Z}\right) df \right\} = \\ &= \int_{-\infty}^{\infty} a(x) \exp\left(i2\pi \frac{x\tilde{r}^{(s)} \Delta f^{(s)}}{\lambda Z}\right) \Phi^{(s)}(x) dx, \end{aligned} \quad (2.4.3)$$

where

$$\Phi^{(s)}(x) = \int_{-\infty}^{\infty} \varphi^{(s)}(f) \exp\left(i2\pi \frac{xf}{\lambda Z}\right) df \quad (2.4.4)$$

is Fourier transform of the sampling device point spread function, or its “frequency response”,  $\{\tilde{\mathbf{r}}^{(s)} = \mathbf{r} + \mathbf{v}^{(s)}\}$  are sample indices shifted as it was explained in Sect. 2.3. Now we can replace the object wave front  $\mathbf{a}(\mathbf{x})$  with its representation

$$\mathbf{a}(\mathbf{x}) = \sum_{k=0}^{N-1} a_k \varphi^{(r)}(\mathbf{x} - \tilde{\mathbf{k}}^{(r)} \Delta \mathbf{x}^{(r)}) \quad (2.4.5)$$

through its samples  $\{a_k\}$ , assuming that  $N$  its samples are available, and that they are indexed from  $k = 0$  to  $k = N - 1$  with  $\{\tilde{\mathbf{k}}^{(r)} = \mathbf{k}^{(r)} + \mathbf{u}^{(r)}\}$  as correspondingly shifted indices. Using in Eq. 2.4.3 the representation of Eq. 2.4.5, we obtain:

$$\begin{aligned} \alpha_r &= \int_{-\infty}^{\infty} \mathbf{a}(\mathbf{x}) \exp\left(i2\pi \frac{\mathbf{x}\tilde{\mathbf{r}}^{(s)}\Delta\mathbf{f}^{(s)}}{\lambda Z}\right) d\mathbf{x} \Phi^{(s)}(\mathbf{x}) = \\ &= \int_{-\infty}^{\infty} \left\{ \sum_{k=0}^{N-1} a_k \varphi^{(r)}(\mathbf{x} - \tilde{\mathbf{k}}^{(r)} \Delta \mathbf{x}^{(r)}) \right\} \exp\left(i2\pi \frac{\mathbf{x}\tilde{\mathbf{r}}^{(s)}\Delta\mathbf{f}^{(s)}}{\lambda Z}\right) d\mathbf{x} \Phi^{(s)}(\mathbf{x}) = \\ &= \left\{ \sum_{k=0}^{N-1} a_k \exp\left(i2\pi \tilde{\mathbf{k}}^{(r)} \tilde{\mathbf{r}}^{(s)} \frac{\Delta \mathbf{x}^{(r)} \Delta \mathbf{f}^{(s)}}{\lambda Z}\right) \right\} \times \\ &= \left\{ \int_{-\infty}^{\infty} \varphi^{(r)}(\mathbf{x}) \Phi^{(s)}(\mathbf{x} + \tilde{\mathbf{k}}^{(s)} \Delta \mathbf{x}^{(r)}) \exp\left(i2\pi \frac{\mathbf{x}\tilde{\mathbf{r}}^{(s)}\Delta\mathbf{f}^{(s)}}{\lambda Z}\right) d\mathbf{x} \right\}. \end{aligned} \quad (2.4.6)$$

As the discrete representation of the integral Fourier transform, only the first multiplier in the product in Eq. 2.4.6 is used:

$$\alpha_r = \sum_{k=0}^{N-1} a_k \exp\left(i2\pi \tilde{\mathbf{k}}^{(r)} \tilde{\mathbf{r}}^{(s)} \frac{\Delta \mathbf{x}^{(r)} \Delta \mathbf{f}^{(s)}}{\lambda Z}\right) \quad (2.4.7)$$

The second multiplier that depends on physical parameters of sampling and reconstruction (display) devices, on sampling intervals and on object-to-hologram distance is ignored. It is this term that, in addition to the approximative signal reconstruction from the final number of its samples as described by Eq. 2.4.5, reflects approximative nature of the discrete representation of integral Fourier transform. The most straightforward way to quantitatively evaluate implication of the approximation is to consider the point spread function and the resolving power of signal Fourier spectrum analysis that can be achieved using Discrete Fourier Transforms. This issue is addressed in Lect. 3.

Sampling intervals in signal and Fourier domains  $\Delta \mathbf{x}^{(r)}$  and  $\Delta \mathbf{f}^{(s)}$  are known to be linked with the “uncertainty relationship”:

$$\Delta \mathbf{x}^{(r)} \geq \frac{\lambda Z}{N \Delta \mathbf{f}^{(s)}} \quad (2.4.8, a)$$

The case

$$\Delta \mathbf{x}^{(r)} = \frac{\lambda Z}{N \Delta \mathbf{f}^{(s)}} \quad (2.4.8, b)$$

associated with the assumption of the “band-limitedness” of signals is referred to as *cardinal sampling*. Depending on relationships between sampling intervals  $\Delta x^{(r)}$  and  $\Delta f^{(s)}$  and on shift parameters  $u^{(s)}$  and  $u^{(r)}$ , the following modifications of the discrete Fourier Transforms outlined in Sects. 2.4.1 – 2.4.5 can be obtained.

#### 2.4.1 1-D direct and inverse Canonical Discrete Fourier Transforms (DFT)

In the assumption that signal and its Fourier spectrum sampling intervals  $\Delta x^{(r)}$  and  $\Delta f^{(s)}$  satisfy the “cardinal” sampling relationship of Eq. 2.4.8, b) and that object signal and object sampling device coordinate systems as well as, those of the hologram and of the hologram sampling device, are, correspondingly, identical and object signal samples  $\{a_k\}$  as well as samples  $\{\alpha_r\}$  of its Fourier hologram are positioned in such a way that samples with indices  $k = 0$  and  $r = 0$  are taken in signal and its Fourier hologram coordinates in points  $x = 0$  and  $f = 0$ , respectively, *Canonical 1-D Discrete Fourier Transforms (DFT)* is obtained:

$$\alpha_r = \frac{1}{\sqrt{N}} \sum_{k=0}^{N-1} a_k \exp\left(i2\pi \frac{kr}{N}\right) \quad (2.4.9, a)$$

One can show that this discrete transform is orthogonal and has inverse transform (IDFT) :

$$a_k = \frac{1}{\sqrt{N}} \sum_{r=0}^{N-1} \alpha_r \exp\left(-i2\pi \frac{kr}{N}\right). \quad (2.4.9, b)$$

Canonical DFT plays a fundamental role in digital signal processing and, in particular, in digital holography and digital image processing thanks to the existence of Fast Fourier Transform (FFT) algorithms. With the use of FFT, computational complexity of transforms is as small as  $O(\log N)$  operations per sample. All discrete transforms considered in this chapter are reducible to DFT and can be computed using FFT algorithms. Thanks to the existence of FFT algorithms, DFT is also very frequently used for fast computation of signal cyclic convolution through the following algorithm:

$$\sum_{n=0}^{N-1} a_n b_{(k-n) \bmod N} = \text{IFFT}_N \{ \text{FFT}_N (\{a_n\}) \bullet \text{FFT}_N (\{b_n\}) \}, \quad (2.4.10)$$

where  $\text{FFT}_N \{\cdot\}$  and  $\text{IFFT}_N \{\cdot\}$  are operators of  $N$ -point FFTs applied to vectors of  $N$  signal samples and symbol  $\bullet$  designates component-wise multiplication of the transform results.

#### 2.4.2 1D direct and inverse Shifted DFTs. Discrete Cosine and Cosine-Sine Transforms

If object and object signal sampling device coordinate systems as well as those of signal spectrum and the spectrum sampling device, are laterally shifted such that signal sample  $\{a_0\}$  and, correspondingly, sample  $\{\alpha_0\}$  of its Fourier spectrum are

taken in signal and spectrum coordinates at points  $\mathbf{x} = \mathbf{u}^{(r)} \Delta \mathbf{x}^{(r)}$  and  $\mathbf{f} = \mathbf{v}^{(s)} \Delta \mathbf{f}^{(s)}$ , respectively, 1-D direct

$$\alpha_r^{u,v} = \frac{1}{\sqrt{N}} \sum_{k=0}^{N-1} a_k \exp\left(i2\pi \frac{\tilde{k}\tilde{r}}{N}\right) \quad (2.4.11, a)$$

and inverse

$$a_k^{u,v} = \frac{1}{\sqrt{N}} \sum_{r=0}^{N-1} \alpha_r^{u,v} \exp\left(-i2\pi \frac{\tilde{k}\tilde{r}}{N}\right) \quad (2.4.11, b)$$

**Shifted DFTs** ( $SDFT(u,v)$ ) are obtained ([2, 3]). The ‘‘cardinal’’ sampling relationship (2.4.8, b) between object signal and its Fourier spectrum sampling intervals  $\Delta \mathbf{x}^{(r)}$  and  $\Delta \mathbf{f}^{(s)}$  is also assumed here.

SDFT can obviously be reduced to DFT and therefore be computed using FFT algorithms. The availability in SDFT of arbitrary shift parameters enables efficient algorithms for hologram reconstruction and object signal re-sampling with sub-pixel accuracy and with the best possible for sampled data discrete sinc-interpolation ([2]). For instance, for  $\mathbf{u}$ -shifted signal re-sampling using SDFT, the following relationship links initial signal samples  $\{a_n\}$  and re-sampled ones  $\{a_k^u\}$ :

$$a_k^u = \sum_{n=0}^{N-1} a_n \frac{\sin[\pi(n-k+u)]}{N \sin[\pi(n-k+u)/N]} = \sum_{n=0}^{N-1} a_n \text{sincd}[N, \pi(n-k+u)], \quad (2.4.12)$$

where

$$\text{sincd}(N; x) = \frac{\sin x}{N \sin x/N} \quad (2.4.13)$$

is the discrete sinc-function (*sincd-function*).

Important special cases of Shifted DFTs are **Discrete Cosine Transform** (DCT)

$$\alpha_r = \sum_{k=0}^{N-1} a_k \cos\left(\pi \frac{k+1/2}{N} r\right) \quad (2.4.14, a)$$

and **Discrete cosine-Sine Transform** (DcST):

$$\alpha_r = \sum_{k=0}^{N-1} a_k \sin\left(\pi \frac{k+1/2}{N} r\right) \quad (2.4.14, b)$$

They are SDFT, with shift parameters 1/2 in the signal domain and 0 in the transform domain, of signals that exhibit even and, correspondingly, odd symmetry ( $\{a_k = \pm a_{2N-1-k}\}$ ). DCT and DcST have fast computational algorithms that belong to the family of fast Fourier Transform algorithms ([2]).

DCT and DcST have numerous applications in image processing and digital holography. In particular, using fast DCT and DCsT algorithms, one can efficiently,

with the complexity of  $O(\log N)$  operations per output sample, implement fast digital convolution with virtually no boundary effects. This allows to substantially alleviate severe boundary effects that are characteristic for using DFT for signal convolution as the DFT based convolution algorithm (Eq. 2.4.10) implements cyclic (periodic) convolution rather than usually required a-periodic convolution. In conclusion of this section note that many other versions of SDFT, DCT and DcST with semi-integer and integer shift parameters can be easily derived for different types of signal and its spectrum symmetries.

### 2.4.3 1D Scaled DFT

If one assumes that sampling rate of either signal samples or spectrum samples or both is  $\sigma$ -times the “cardinal” sampling rate ( $\Delta x^{(r)} = \lambda Z / \sigma N \Delta f^{(s)}$ ), and that signal and its Fourier hologram samples  $\{a_0\}$  and  $\{\alpha_0\}$  are positioned with shifts  $(u^{(r)}, v^{(s)})$  with respect to the origin of the corresponding signal and spectrum coordinate systems, *Scaled DFT (ScDFT)*

$$\alpha_r^\sigma = \frac{1}{\sqrt{\sigma N}} \sum_{k=0}^{N-1} a_k \exp\left(i2\pi \frac{\tilde{k}\tilde{r}}{\sigma N}\right) \quad (2.4.15,a)$$

is obtained. Modification of this transform for zero shift parameters is also known under the names of “*chirp z-transform*” ([4,5]) and “*fractional discrete Fourier transform*”. The first name is associated with the way to compute it efficiently (see below Eq. 2.4.16). The second name assumes that it is a discretized version of the fractional integral Fourier transform ([6,7]) that has found some applications in optics and quantum mechanics. We prefer the name “Scaled DFT” because it is more intuitive, refers to its physical interpretation and fits the entire nomenclature of discrete Fourier transforms (shifted, scaled, rotated, scaled and rotated, affine) introduced in this lecture.

Scaled DFT has its inverse only if  $\sigma N$  is an integer number ( $\sigma N \in Z$ ) and  $\sigma > 1$  (see Appendix A1.). In this case, the inverse ScDFT is defined as

$$a_k^\sigma = \frac{1}{\sqrt{\sigma N}} \sum_{r=0}^{\sigma N-1} \alpha_r \left(-i2\pi \frac{\tilde{k}\tilde{r}}{\sigma N}\right) = \begin{cases} a_k, & k = 0, 1, \dots, N-1 \\ 0, & k = N, N+1, \dots, \sigma N-1 \end{cases} \quad (2.4.15,b)$$

For computational purposes, it is convenient to represent ScDFT as a cyclic convolution

$$\begin{aligned} \alpha_r^\sigma &= \frac{1}{\sqrt{\sigma N}} \sum_{k=0}^{N-1} a_k \exp\left(i2\pi \frac{\tilde{k}\tilde{r}}{\sigma N}\right) = \\ &= \frac{\exp\left(i\pi \frac{\tilde{r}^2}{\sigma N}\right)}{\sqrt{\sigma N}} \sum_{k=0}^{N-1} \left[ a_k \exp\left(i\pi \frac{\tilde{k}^2}{\sigma N}\right) \right] \exp\left[-i\pi \frac{(\tilde{k}-\tilde{r})^2}{\sigma N}\right], \end{aligned} \quad (2.4.16)$$

that can be computed using FFT algorithm as following:

$$\alpha_r^{(\sigma)} = \text{IFFT}_{\lfloor \sigma N \rfloor} \left\{ \text{ZP}_{\lfloor \sigma N \rfloor} \left[ \text{FFT}_N \left\{ a_k \exp \left( i\pi \frac{\tilde{k}^2}{\sigma N} \right) \right\} \right] \bullet \text{FFT}_{\lfloor \sigma N \rfloor} \left\{ \exp \left( -i\pi \frac{\tilde{n}^2}{\sigma N} \right) \right\} \right\}, \quad (2.4.17)$$

where  $\text{FFT}_M \{\cdot\}$  and  $\text{IFFT}_M \{\cdot\}$  denote  $M$ -point direct and inverse FFTs,  $\lfloor \sigma N \rfloor$  is an integer number defined by the inequality  $\sigma N \leq \lfloor \sigma N \rfloor < \sigma N + 1$ , and  $\text{ZP}_M[\cdot]$  is a zero-padding operator. If  $\sigma > 1$ , it pads the array of  $N$  samples with zeros to the array of  $\lfloor \sigma N \rfloor$  samples. If  $\sigma < 1$ , it cuts array of  $N$  samples to size of  $\lfloor \sigma N \rfloor$  samples.

The availability in ScDFT of the arbitrary scale parameter enables signal discrete-sinc-interpolated re-sampling and Fourier hologram reconstruction in an arbitrary scale. For instance, if one computes canonical DFT of a signal and then applies to the obtained spectrum scaled IDFT with a scale parameter  $\sigma$ , discrete sinc-interpolated samples of the initial signal in a scaled coordinate system will be obtained:

$$a_k^\sigma = \sum_{n=0}^{N-1} a_n \text{sincd}[N; \pi(n - k/\sigma)], \quad (2.4.18)$$

If  $\sigma > 1$ , signal  $\{a_k\}$  is sub-sampled (its discrete representation is zoomed in) with discrete sinc-interpolation and the sub-sampled signal retains the initial signal bandwidth. If  $\sigma < 1$ , signal  $\{a_k\}$  is down-sampled (decimated). For signal down-sampling, an appropriate signal low-pass filtering required to avoid aliasing artifacts is automatically carried out by the imbedded zero-padding operator  $\text{ZP}_{\lfloor \sigma N \rfloor}$ .

#### 2.4.4 2D Canonical Separable DFTs.

In order to introduce discrete representation of 2-D intergral transforms, one should specify a 2-D sampling grid. Most frequently, rectangular sampling grid is assumed for sampled representation of 2-D signals. In this case, for 2-D integral Fourier Transform, the following separable 2-D canonical direct and inverse DFTs:

$$\alpha_{r,s} = \frac{1}{\sqrt{N_1 N_2}} \sum_{k=0}^{N_1-1} \exp \left( i2\pi \frac{kr}{N_1} \right) \sum_{l=0}^{N_2-1} a_{k,l} \exp \left( i2\pi \frac{ls}{N_1} \right); \quad (2.4.19,a)$$

$$a_{k,l} = \frac{1}{\sqrt{N_1 N_2}} \sum_{r=0}^{N_1-1} \exp \left( -i2\pi \frac{kr}{N_1} \right) \sum_{s=0}^{N_2-1} \alpha_{r,s} \exp \left( -i2\pi \frac{ls}{N_2} \right). \quad (2.4.19, b)$$

are obtained in the assumption that object signal and its hologram sampling and reconstruction are performed in rectangular sampling grids (row-wise, column-wise) collinear with the object coordinate system. Here  $N_1$  and  $N_2$  are dimensions of 2-D arrays of signal and its Fourier spectrum samples. In separable 2-D DFTs, 1-D Shifted and Scaled DFTs can also be used to enable signal 2-D separable discrete sinc-interpolated resampling and re-scaling.

### 2.4.5 2-D Rotated and Affine DFTs.

In 2-D case, a natural generalization of 1-D Shifted and Scaled DFTs is 2-D *Affine DFT (AffDFT)*. AffDFT is obtained in the assumption that either signal or its spectrum sampling or reconstructions are carried out in affine transformed, with respect to signal/spectrum coordinate systems  $(x, y)$ , coordinates  $(\tilde{x}, \tilde{y})$ :

$$\begin{bmatrix} x \\ y \end{bmatrix} = \begin{bmatrix} A & B \\ C & D \end{bmatrix} \begin{bmatrix} \tilde{x} \\ \tilde{y} \end{bmatrix} \quad (2.4.20)$$

With  $\sigma_A = \lambda Z / N_1 A \Delta \tilde{x} \Delta f_x$ ;  $\sigma_B = \lambda Z / N_2 B \Delta \tilde{y} \Delta f_x$ ;  $\sigma_C = \lambda Z / N_1 C \Delta \tilde{x} \Delta f_y$ ,  $\sigma_D = \lambda Z / N_2 D \Delta \tilde{y} \Delta f_y$ , where  $\Delta \tilde{x}$ ,  $\Delta \tilde{y}$ ,  $\Delta f_x$  and  $\Delta f_y$  are object and its Fourier hologram sampling intervals in object  $(\tilde{x}, \tilde{y})$  and hologram  $(f_x, f_y)$  planes, AffDFT is defined as

$$\alpha_{r,s} = \sum_{k=0}^{N_1-1} \sum_{l=0}^{N_2-1} a_{k,l} \exp \left[ i2\pi \left( \frac{\tilde{r}k}{\sigma_A N_1} + \frac{\tilde{s}k}{\sigma_C N_1} + \frac{\tilde{r}l}{\sigma_B N_2} + \frac{\tilde{s}l}{\sigma_D N_2} \right) \right], \quad (2.4.21)$$

where  $\{\tilde{k}, \tilde{l}\}$  and  $\{\tilde{r}, \tilde{s}\}$  are biased (shifted) sampling indices in object and hologram planes as it is explained in Eq. 2.3.1.

A special case of affine transforms is rotation. For rotation angle  $\theta$ :

$$\begin{bmatrix} x \\ y \end{bmatrix} = \begin{bmatrix} \cos \theta & \sin \theta \\ -\sin \theta & \cos \theta \end{bmatrix} \begin{bmatrix} \tilde{x} \\ \tilde{y} \end{bmatrix} \quad (2.4.22)$$

With  $N_1 = N_2 = N$ ,  $\Delta \tilde{x} = \Delta \tilde{y} = \Delta x$ ,  $\Delta f_x = \Delta f_y = \Delta f$ , and  $\Delta x \Delta f = \lambda Z / N$  (cardinal sampling), 2-D *Rotated DFT (RotDFT)* can be obtained as

$$\alpha_{r,s}^\theta = \frac{1}{\sigma N} \sum_{k=0}^{N-1} \sum_{l=0}^{N-1} a_{k,l} \exp \left[ i2\pi \left( \frac{\tilde{k} \cos \theta + \tilde{l} \sin \theta}{N} \tilde{r} - \frac{\tilde{k} \sin \theta - \tilde{l} \cos \theta}{N} \tilde{s} \right) \right]. \quad (2.4.23)$$

An obvious generalization of RotDFT is *Rotated and Scaled RotDFT (RotScDFT)*:

$$\alpha_{r,s}^\theta = \frac{1}{\sigma N} \sum_{k=0}^{N-1} \sum_{l=0}^{N-1} a_{k,l} \exp \left[ i2\pi \left( \frac{\tilde{k} \cos \theta + \tilde{l} \sin \theta}{\sigma N} \tilde{r} - \frac{\tilde{k} \sin \theta - \tilde{l} \cos \theta}{\sigma N} \tilde{s} \right) \right] \quad (2.4.24)$$

that assumes 2-D signal sampling in  $\theta$ -rotated and  $\sigma$ -scaled coordinate systems. Similarly to ScDFT, RotScDFT can be reduced to 2-D cyclic convolution using identities:

$$\begin{aligned} \alpha_{r,s}^\theta &= \frac{1}{\sigma N} \sum_{k=0}^{N-1} \sum_{l=0}^{N-1} \tilde{a}_{k,l} \exp \left[ i2\pi \left( \frac{\tilde{k} \cos \theta + \tilde{l} \sin \theta}{\sigma N} \tilde{r} - \frac{\tilde{k} \sin \theta - \tilde{l} \cos \theta}{\sigma N} \tilde{s} \right) \right] = \\ &= \frac{1}{\sigma N} \sum_{k=0}^{N-1} \sum_{l=0}^{N-1} \tilde{a}_{k,l} \exp \left[ i2\pi \left( \frac{\tilde{k} \tilde{r} + \tilde{l} \tilde{s}}{\sigma N} \cos \theta + \frac{\tilde{l} \tilde{r} - \tilde{k} \tilde{s}}{\sigma N} \sin \theta \right) \right] \end{aligned} \quad (2.4.25)$$

$$2(\tilde{k} \tilde{r} + \tilde{l} \tilde{s}) = \tilde{r}^2 + \tilde{k}^2 - \tilde{s}^2 - \tilde{l}^2 - (\tilde{r} - \tilde{k})^2 + (\tilde{s} + \tilde{l})^2; \quad (2.4.26)$$

$$2(\tilde{l}\tilde{r} - \tilde{k}\tilde{s}) = 2\tilde{k}\tilde{l} - 2\tilde{r}\tilde{s} + 2(\tilde{r} - \tilde{k})(\tilde{s} + \tilde{l}). \quad (2.4.27)$$

Inserting Eqs. 2.4.26 and 2.4.27 into Eq. 2.4.25, obtain:

$$\begin{aligned} \alpha_{r,s}^\theta &= \frac{1}{\sigma N} \sum_{r=0}^{N-1} \sum_{s=0}^{N-1} \tilde{a}_{k,l} \exp \left[ i2\pi \left( \frac{\tilde{k}\tilde{r} + \tilde{l}\tilde{s}}{\sigma N} \cos \theta + \frac{\tilde{l}\tilde{r} - \tilde{k}\tilde{s}}{\sigma N} \sin \theta \right) \right] = \\ &= \frac{1}{\sigma N} \sum_{k=0}^{N-1} \sum_{l=0}^{N-1} \tilde{a}_{k,l} \exp \left[ i\pi \frac{\tilde{r}^2 + \tilde{k}^2 - \tilde{s}^2 - \tilde{l}^2 - (\tilde{r} - \tilde{k})^2 + (\tilde{s} + \tilde{l})^2}{\sigma N} \cos \theta \right] \times \\ &= \exp \left[ -i2\pi \frac{2\tilde{k}\tilde{l} - 2\tilde{r}\tilde{s} + 2(\tilde{r} - \tilde{k})(\tilde{s} + \tilde{l})}{\sigma N} \sin \theta \right] = \\ &= \left\{ \frac{1}{\sigma N} \sum_{k=0}^{N-1} \sum_{l=0}^{N-1} (\alpha_{r,s} A_{r,s}) \text{ChF}(\tilde{s} + \tilde{l}, \tilde{r} - \tilde{k}) \right\} \exp \left[ -i\pi \frac{(\tilde{r}^2 - \tilde{s}^2) \cos \theta - 2\tilde{r}\tilde{s} \sin \theta}{\sigma N} \right], \end{aligned} \quad (2.4.28)$$

where

$$\text{ChF}(\tilde{s} + \tilde{l}, \tilde{r} - \tilde{k}) = \exp \left[ i\pi \frac{(\tilde{s} + \tilde{l})^2 \cos \theta - (\tilde{r} - \tilde{k})^2 \cos \theta - 2(\tilde{r} - \tilde{k})(\tilde{s} + \tilde{l}) \sin \theta}{\sigma N} \right]; \quad (2.4.29, a)$$

and

$$A_{r,s} = \left\{ \exp \left[ -i\pi \frac{(\tilde{r}^2 - \tilde{s}^2) \cos \theta + 2\tilde{r}\tilde{s} \sin \theta}{\sigma N} \right] \right\}. \quad (2.4.29, b)$$

The convolution defined by Eq. 2.4.28 can be efficiently computed using FFT as:

$$\{\tilde{a}_{k,l}\} = \text{IFFT}_{2_{\lfloor \sigma N \rfloor}} \left\{ \text{FFT}_{2_{\lfloor \sigma N \rfloor}} \left[ \text{ZP}_{\lfloor N\sigma \rfloor} \left[ \text{FFT}_{2_N} (a_{k,l}) \right] \bullet A_{r,s} \right] \bullet \text{FFT}_{2_{\lfloor \sigma N \rfloor}} [\text{ChF}(r,s)] \right\}, \quad (2.4.30)$$

where  $\text{FFT}_{2_{\lfloor N\sigma \rfloor}}[\cdot]$  and  $\text{IFFT}_{2_{\lfloor N\sigma \rfloor}}[\cdot]$  are operators of direct and inverse  $\lfloor N\sigma \rfloor$ -point 2D FFT,  $\lfloor N\sigma \rfloor$  is the smallest integer larger than  $N\sigma$ ,  $\text{ZP}_{\lfloor N\sigma \rfloor}[\cdot]$  is a 2-D zero-padding operator. For  $\sigma > 1$ , it pads array of  $N \times N$  samples with zeros to the array of  $\lfloor \sigma N \rfloor \times \lfloor \sigma N \rfloor$  samples with  $\lfloor \sigma N \rfloor$  defined, as above, by the inequality  $\sigma N \leq \lfloor \sigma N \rfloor < \sigma N + 1$ . For  $\sigma < 1$ , the padding operator cuts array of  $N \times N$  samples to the size of  $\lfloor \sigma N \rfloor \times \lfloor \sigma N \rfloor$  samples.

## 2.5. Discrete Fresnel transforms

In this section, we outline discrete transforms and their fast algorithms that can be used for numerical evaluation of the “near zone” (Fresnel) diffraction integral. Using above described principles of discretization of signal transforms one can obtain its following discrete representations.

### 2.5.1. Canonical Discrete Fresnel Transform

Similarly to Canonical DFT, direct and inverse *Canonical Discrete Fresnel Transforms (CDFrT)*

$$\alpha_r = \frac{1}{\sqrt{N}} \sum_{k=0}^{N-1} a_k \exp \left[ i\pi \frac{(k\mu - r/\mu)^2}{N} \right] \quad (2.5.1, a)$$

and

$$a_k = \frac{1}{\sqrt{N}} \sum_{r=0}^{N-1} \alpha_r \exp \left[ -i\pi \frac{(k\mu - r/\mu)^2}{N} \right] \quad (2.5.1, b)$$

are obtained as a discrete representation of the integral Fresnel transform (Eq. 2.4) in the assumption of the cardinal sampling relationship  $\Delta \mathbf{x}^{(r)} = \lambda \mathbf{Z} / N \Delta \mathbf{f}^{(s)}$  between sampling intervals in signal and transform domains and of zero shifts of object and hologram sampling grids with respect to the corresponding coordinate systems. Parameter  $\mu^2$  in Eqs. 2.5.1 is defined as

$$\mu^2 = \lambda \mathbf{Z} / N \Delta \mathbf{f}^2 \quad (2.5.1, c)$$

It plays in DFrT a role of a distance (focusing) parameter.

CDFrT can readily be expressed via DFT:

$$\alpha_r = \frac{1}{\sqrt{N}} \left\{ \sum_{k=0}^{N-1} \left[ a_k \exp \left( i\pi \frac{k^2 \mu^2}{N} \right) \right] \exp \left( -i2\pi \frac{kr}{N} \right) \right\} \exp \left( i\pi \frac{r^2}{\mu^2 N} \right) \quad (2.5.2)$$

and, therefore, can be computed using FFT algorithms. In numerical reconstruction of Fresnel holograms, this method for computing DFrT is known as the “*Fourier reconstruction algorithm*”.

### 2.5.2. Shifted Discrete Fresnel Transforms

If one assumes cardinal sampling condition and arbitrary shift parameters in object and/or its hologram sampling, *Shifted Discrete Fresnel Transforms (SDFrT)*

$$\alpha_r^{(\mu, w)} = \frac{1}{\sqrt{N}} \sum_{k=0}^{N-1} a_k \exp \left[ -i\pi \frac{(k\mu - r/\mu + w)^2}{N} \right] \quad (2.5.3)$$

are obtained. Parameter  $w$  in Eq. 2.5.3 is a joint shift parameter that unifies shifts  $u^{(r)}$  and  $v^{(s)}$  of sampling grids in object and hologram planes:

$$w = u^{(r)}/\mu - v^{(s)}\mu. \quad (2.5.4)$$

### 2.5.3. Focal Plane Invariant Discrete Fresnel Transform

Because shift parameter  $w$  in Shifted DFrT is a combination of shifts in object and hologram planes, shift in object plane causes a corresponding shift in Fresnel hologram plane, which, however, depends, according to Eq. 2.5.4, on the focusing parameter  $\mu$ . One can break this interdependence if, in the definition of the discrete representation of integral Fresnel transform, impose a symmetry condition

$\alpha_r^{(\mu,w)} = \alpha_{N-r}^{(\mu,w)}$  for the transform  $\alpha_r^{(\mu,w)} = \exp\left[-i\pi \frac{(r/\mu - w)^2}{N}\right]$  of a point source

$\delta(k) = 0^k$ ,  $k = 0, 1, \dots, N-1$ . This condition is satisfied when  $w = N/2\mu$ , and SDFrT for such a shift parameter takes form:

$$\alpha_r^{(\mu, \frac{N}{2\mu})} = \frac{1}{\sqrt{N}} \sum_{k=0}^{N-1} a_k \exp\left\{-i\pi \frac{[k\mu - (r - N/2)/\mu]^2}{N}\right\}. \quad (2.5.5)$$

We refer to this discrete transform as to **Focal Plane Invariant Discrete Fresnel Transform (FPIDFrT)**. In numerical reconstruction of holograms, position of the reconstructed object in the output sampling grid depends on the object-hologram distance when canonical DFrT is used. FPIDFrT defined by Eq. (2.5.4) allows keeping position of reconstructed objects invariant to the object-hologram distance ([8]), which might be useful in applications. In particular, invariance of the reconstruction object position with respect to the distance parameter can ease automatic object focusing and usage of pruned FFT algorithms ([1]) in reconstruction of a part of the field of view.

Figs. 2.1 and 2.2 adopted from Ref. [8] illustrate results of reconstruction of two types of digital holograms in different focal planes. Images a) -c) were obtained using conventional Discrete Fresnel transform defined by Eq. 2.5.2. Images in d) -f) were obtained using Focal Plane Invariant Discrete Fresnel transform defined by Eq. 2.5.5<sup>1</sup>.

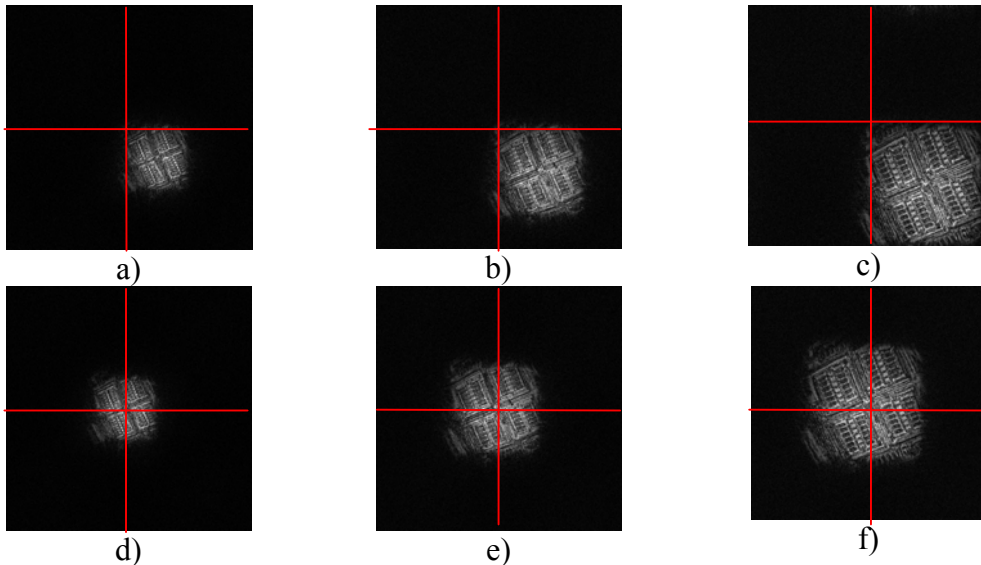


Fig. 2.1. Reconstruction of a hologram on different depth using Discrete Fresnel Transform (a) –c)) and using Focal Plane Invariant Discrete Fresnel Transform (d) – f)). (Hologram was kindly provided by Dr. G. Pedrini ([9]))

<sup>1</sup> See also hologr\_reconstr\_demo.m;

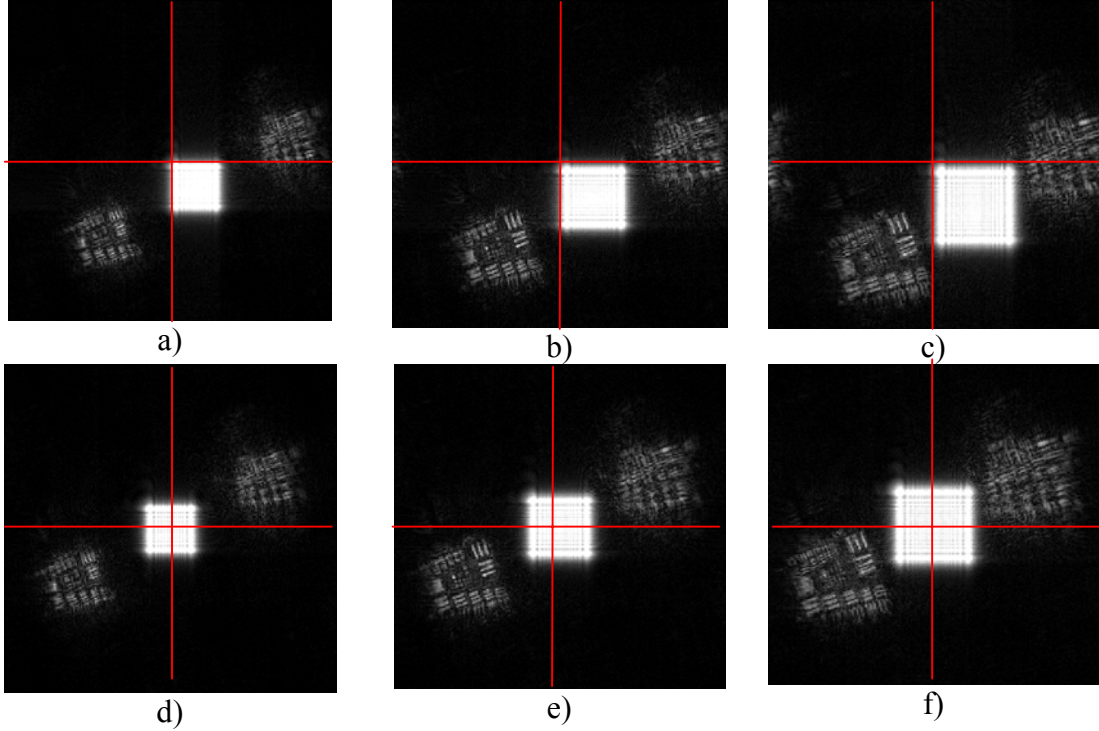


Fig. 2.2. Reconstruction of an off axis hologram. a) - c): reconstruction on different depth using Discrete Fresnel Transform (Eq.); d) - f) - reconstruction using Focal Plane Invariant Discrete Fresnel Transform. The hologram was copied from a PDF file of paper ([10])

#### 2.5.4. Partial Discrete Shifted Fresnel Transform

When, in hologram reconstruction, only intensity of the object wavefront is required, direct and inverse *Partial Discrete Fresnel Transforms* (PDFrT)

$$\hat{\alpha}_r^{(\mu, \nu)} = \frac{1}{\sqrt{N}} \sum_{k=0}^{N-1} a_k \exp\left(-i\pi \frac{k^2 \mu^2}{N}\right) \exp\left[i2\pi \frac{k(r - w\mu)}{N}\right]; \quad (2.5.6, a)$$

$$a_k^{(\mu, \nu)} = \frac{1}{\sqrt{N}} \sum_{r=0}^{N-1} \hat{\alpha}_r^{(\mu, \nu)} \exp\left[-i2\pi \frac{(r - w\mu)k}{N}\right] \exp\left(i\pi \frac{k^2 \mu^2}{N}\right). \quad (2.5.6, b)$$

can be used as discrete representations of the integral Fresnel Transform. They are obtained by removing, from Eqs. 2.5.3 exponential phase terms that do not depend on signal sampling index  $k$ . As one can see from Eqs. 2.5.6, direct and inverse PDFrT are essentially versions of SDFT.

### 2.5.5. Invertibility of Discrete Fresnel Transforms and frinced-function

For shifted shift and focusing parameters, Discrete Fresnel Transforms are invertible orthogonal transforms. If, however, one computes, for a discrete signal  $\{a_k\}$ ,  $k = 0, 1, \dots, N-1$ , direct SDFrT with parameters  $(\mu_+, w_+)$  and then inverts it with inverse SDFrT with parameters  $(\mu_-, w_-)$ , the following result, different from  $\{a_k\}$ , will be obtained:

$$a_k^{(\mu^\pm, w^\pm)} = \frac{\exp\left[-i\pi \frac{(k\mu_- + w_-)^2}{N}\right]}{N} \times \sum_{n=0}^{N-1} a_n \exp\left[i\pi \frac{(n\mu_+ + w_+)^2}{N}\right] \text{frinced}(N; q; n - k + \bar{w}_\pm + qN/2) \quad (2.5.7)$$

where

$$\text{frinced}(N; q; x) = \frac{1}{N} \sum_{r=0}^{N-1} \exp\left(i\pi \frac{qr^2}{N}\right) \exp\left(-i2\pi \frac{xr}{N}\right). \quad (2.5.8, a)$$

and  $q = 1/\mu_+^2 - 1/\mu_-^2$ ;  $\bar{w}_\pm = \bar{w}_+/\mu_+ - \bar{w}_-/\mu_-$ . It is a function analogous to the sincd-function of the DFT (Eq. 2.3.13) and identical to it when  $q = 0$ . We refer to this function as to *frinced-function*. In numerical reconstruction of holograms, frinced-function is the convolution kernel that links object and its “out of focus” reconstruction.

Focal plane invariant version of frinced- function is obtained as

$$\overline{\text{frinced}}(N; q; x) = \frac{1}{N} \sum_{r=0}^{N-1} \exp\left[i\pi \frac{qr(r-N)}{N}\right] \exp\left(-i2\pi \frac{xr}{N}\right) \quad (2.5.8, b)$$

Fig. 2.3 illustrates behavior of absolute values of function  $\overline{\text{frinced}}(N; q; x)$  for different values of  $q$  in the range  $0 \leq q \leq 1$ . In Fig. 2.3, absolute values of function  $\sqrt{q \overline{\text{frinced}}(N; q; x)}$  for  $q$  in the range  $0 \leq q \leq 2.5$  are shown as an image in coordinates  $(q, x)$  to demonstrate aliasing artifacts that appear  $q > 1$ .

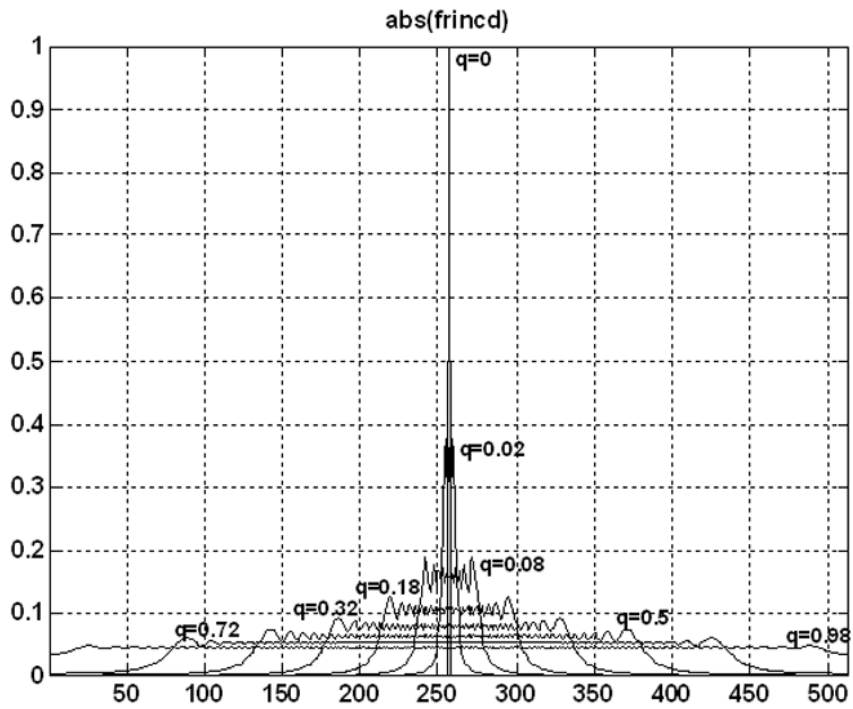


Fig.2. 3. Absolute values of function  $\overline{\text{frincd}}(N; q; x)$  for several values of  $q$ .

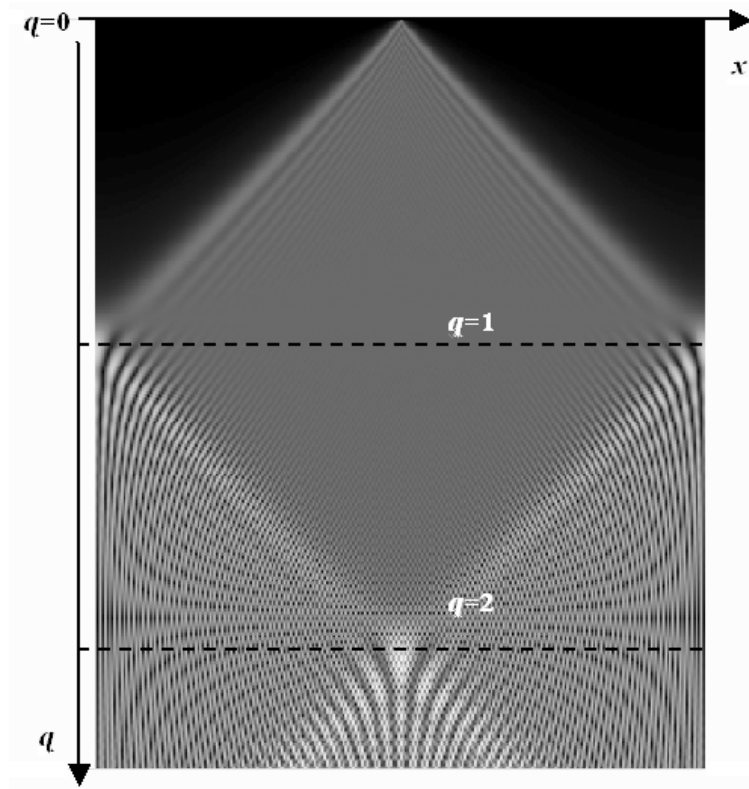


Fig. 2.4. Function  $\sqrt{q \text{frincd}}(N; q; x)$  represented, in coordinates  $(q, x)$ , as an image with lightness proportional to its absolute values. Note aliasing artifacts for  $q > 1$  that culminate when  $q \geq 2$

As one can see from Eqs. 2.5.8, fringed-function is DFT of a chirp-function. It is known that integral Fourier transform of a chirp-function is also a chirp-function. In Appendix A2.1 it is shown that, in distinction from the continuous case, fringed-function can only be approximated by a chirp-function:

$$\mathbf{fringed}(N;\pm q;x) \cong \sqrt{\frac{\pm i}{Nq}} \exp\left[\mp i\pi \frac{x^2}{qN}\right] \mathbf{rect}\left[\frac{x}{q(N-1)}\right] \quad (2.5.9, a)$$

For  $q = 1$  and integer  $x$ , it is reduced to an exact chirp-function

$$\mathbf{fringed}(N;1;x) = \sqrt{\frac{i}{N}} \exp\left(-i\pi \frac{x^2}{N}\right). \quad x \in \mathbf{Z} \quad (2.5.9, b)$$

As it was already indicated, for  $q = 0$  fringed-function reduces to sincd-function:

$$\mathbf{fringed}(N;0;x) = \mathbf{sincd}(N;\pi x) \exp\left(-i\pi \frac{N-1}{N} x\right) \quad (2.5.9, c)$$

Movies in Fig. 5 illustrate numerical reconstruction of Fresnel holograms on different scene depths using Focal Plane Invariant Discrete Fresnel Transform.

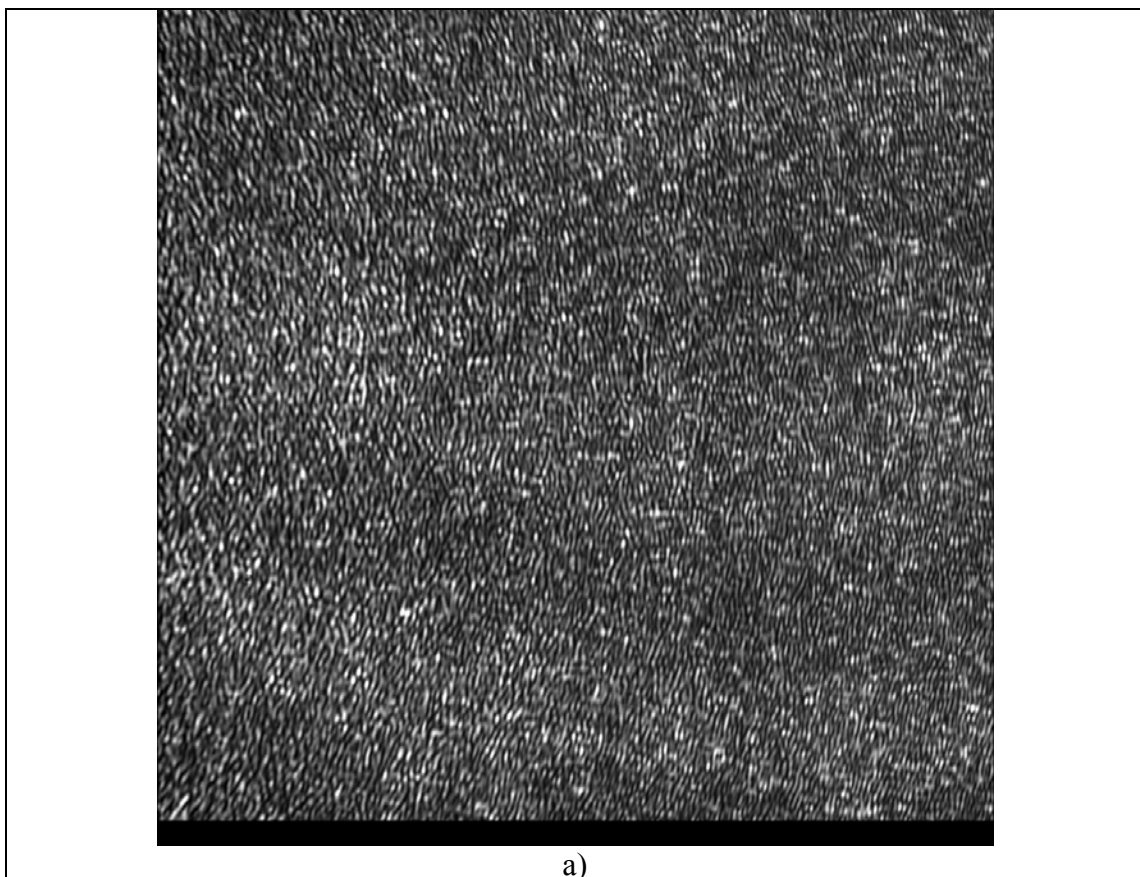


Fig. 2.5 a) Digitally recorded hologram BIAS

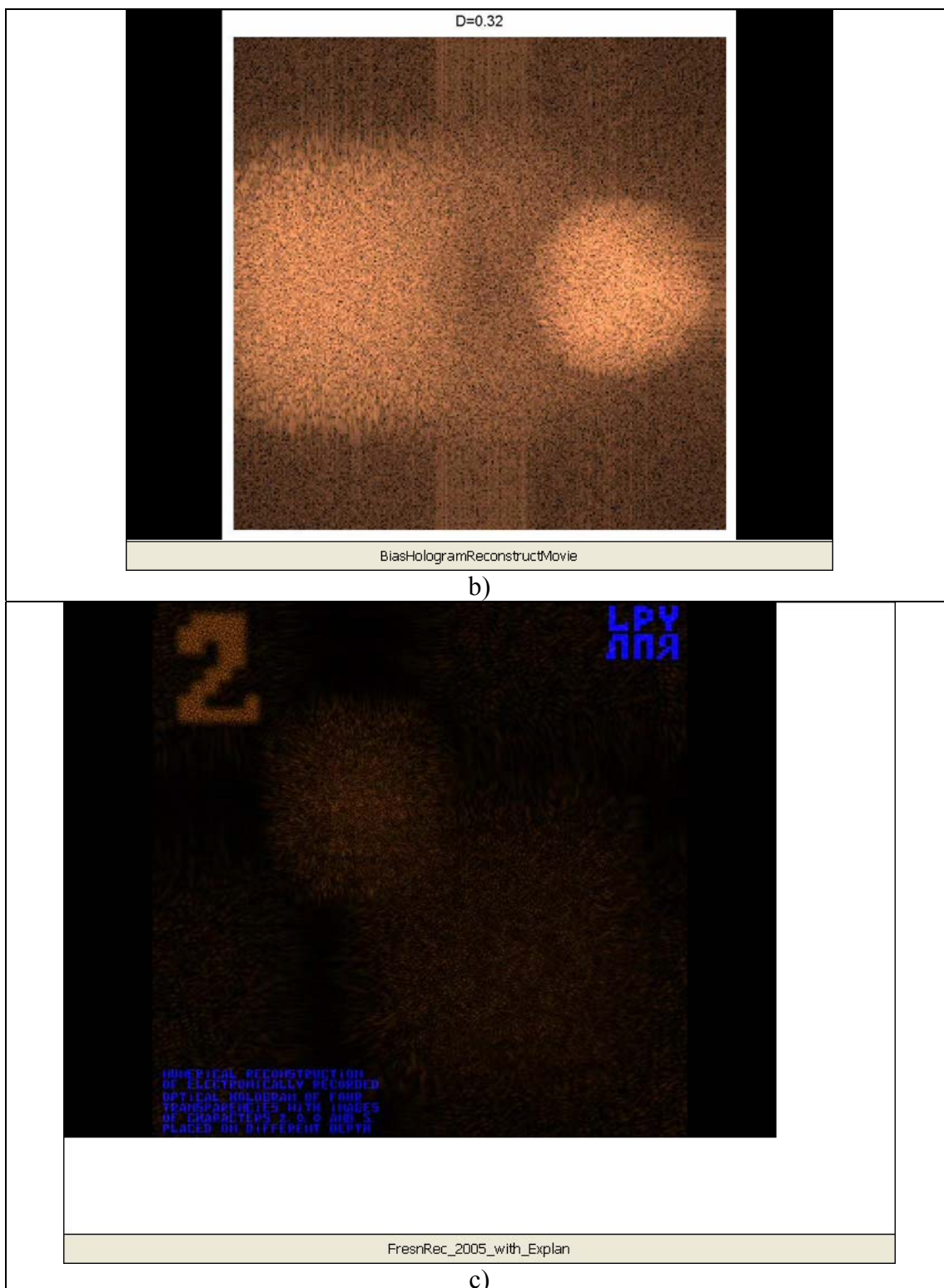


Fig. 2.5. Illustrative movies that demonstrate BIAS hologram reconstruction on different depths: b) – reconstruction of an off-axis recorded hologram of a die; c) reconstruction of simulated computer-generated hologram of 4 numerical characters placed under different angle of view on different scene depths

### 2.5.6. Convolutional Discrete Fresnel Transform

For small distances  $Z$ , canonical Discrete Fresnel Transform and its above-described versions face aliasing problems when focusing parameter  $\mu^2 = \lambda Z / N \Delta f^2$  is becoming less than 1, or correspondingly, parameter  $q$  of the fringed-function is larger than 1. For such cases, discrete representation of integral Fresnel transform can be used that is built on the base of the angular spectrum propagation version of the integral Fresnel Transform (Eq. 2.2.6):

$$\begin{aligned} \alpha(f) \propto & \int_{-\infty}^{\infty} \left[ \int_{-\infty}^{\infty} a(x) \exp(i2\pi x \xi) dx \right] \exp(-i\pi \lambda Z \xi^2) \exp(-i2\pi f \xi) d\xi = \\ & \int_{-\infty}^{\infty} \int_{-\infty}^{\infty} a(x) \exp[i2\pi(x-f)\xi] \exp(-i\pi \lambda Z \xi^2) dx d\xi \end{aligned} \quad (2.5.10)$$

and in the deliberate assumption that sampling intervals  $\Delta x^{(r)}$  and  $\Delta f^{(s)}$  of the object signal and its Fresnel transform are identical:  $\Delta x^{(r)} = \Delta f^{(s)}$ . In this assumption, the following version of discrete Fresnel Transform referred to as **Convolutional Discrete Fresnel Transform (ConvDFrT)** is obtained for object and hologram sampling shift parameters  $u^{(r)}$  and  $v^{(s)}$ :

$$\begin{aligned} \alpha_r = & \frac{1}{N} \sum_{s=0}^{N-1} \left[ \sum_{k=0}^{N-1} a_k \exp\left(i2\pi \frac{k-r+w}{N} s\right) \right] \exp\left(-i\pi \frac{\mu^2 s^2}{N}\right) = \\ & \frac{1}{N} \sum_{k=0}^{N-1} a_k \left[ \sum_{s=0}^{N-1} \exp\left(-i\pi \frac{\mu^2 s^2}{N}\right) \exp\left(i2\pi \frac{k-r+w}{N} s\right) \right], \end{aligned} \quad (2.5.11, a)$$

or

$$\alpha_r = \sum_{k=0}^{N-1} a_k \text{frinced}^*(N; \mu^2; k-r+w) \quad (2.5.11, b)$$

where  $w = u^{(r)} - v^{(s)}$  and asterisk denotes complex conjugate

ConvDFrT, similarly to DFTs and DFrTs, is an orthogonal transform with inverse **ConvDFrT** defined as

$$\begin{aligned} a_k = & \frac{1}{N} \sum_{s=0}^{N-1} \left[ \sum_{r=0}^{N-1} \alpha_r \exp\left(-i2\pi \frac{k-r+w}{N} s\right) \right] \exp\left(i\pi \frac{\mu^2 s^2}{N}\right) = \\ & \sum_{r=0}^{N-1} \alpha_r \text{frinced}(N; \mu^2; k-r+w). \end{aligned} \quad (2.5.11, c)$$

When  $\mu^2 = 0$  and  $w = 0$ , ConvDFrT degenerates to the identical transform.

Although ConvDFrT as a discrete transform can be inverted for any  $\mu^2$ , in numerical reconstruction of holograms it can be recommended only for

$\mu^2 = \lambda Z / N \Delta f^2 \leq 1$ . If  $\mu^2 = \lambda Z / N \Delta f^2 > 1$ , aliasing appears in form of overlapping periodical copies of the reconstruction result.

### 2.5.7. 2-D Discrete Fresnel Transforms. Scaled and rotated transforms

2-D discrete Fresnel Transforms are usually defined as separable row-column transforms. For instance, canonical 2-D Fresnel Transform is defined as

$$\alpha_{r,s}^{(\mu,0,0)} = \frac{1}{\sqrt{N_1 N_2}} \sum_{k=0}^{N_1-1} \exp \left[ -i\pi \frac{(k\mu - r / \mu)^2}{N} \right] \sum_{l=0}^{N_2-1} a_{k,l} \exp \left[ -i\pi \frac{(l\mu - s / \mu)^2}{N_2} \right]. \quad (2.5.12)$$

As the last stage in the algorithmic implementations of all versions of discrete Fresnel transforms is Discrete Fourier Transform implemented via FFT algorithm, scaled and rotated modification of DFT can be applied at this stage. This will enable scaling and/or rotation of the transform result, if they are required when using Discrete Fresnel transforms for numerical reconstruction of digitally recorded holograms. For instance, scaled reconstruction is required in reconstruction of hologram of the same object recorded in different wavelength, such as color holograms.

## 2.6. Discrete Kirchhoff-Rayleigh-Sommerfeld transforms

Using the above-described transform discretization principles and assuming, as in the case of the Convolutional Fresnel Transform, identical sampling intervals  $\Delta \mathbf{x}^{(r)}$  and  $\Delta \mathbf{f}^{(s)}$  of the signal and its transform, one can obtain the following 1-D and 2-D (for square data arrays) discrete representations of integral Kirchhoff-Rayleigh-Sommerfeld transform:

$$\alpha_r = \sum_{k=0}^{N-1} a_k \mathbf{DKRS}^{(1D)}(\tilde{k} - \tilde{r}) \quad (2.6.1)$$

and

$$\alpha_{r,s} = \sum_{k=0}^{N-1} \sum_{l=0}^{N-1} a_{k,l} \mathbf{DKRS}^{(2D)}(\tilde{k} - \tilde{r}; \tilde{l} - \tilde{r}) \quad (2.6.2)$$

where it is denoted:

$$\mathbf{DKRS}_{\tilde{z}, \mu}^{(1D)}(n) = \frac{\exp \left[ i2\pi \frac{\tilde{z}^2 \sqrt{1 + n^2 / \tilde{z}^2}}{\mu^2 N} \right]}{1 + n^2 / \tilde{z}^2}; \quad (2.6.3, a)$$

$$DKRS_{\tilde{z},\mu}^{(2D)}(m,n) = \frac{\exp\left[i2\pi \frac{\tilde{z}^2 \sqrt{1+m^2/\tilde{z}^2 + n^2/\tilde{z}^2}}{\mu^2 N}\right]}{1+m^2/\tilde{z}^2 + n^2/\tilde{z}^2}; \quad (2.6.3, b)$$

$$\tilde{z} = Z/\Delta f; \quad \mu^2 = \frac{\lambda Z}{N\Delta f^2} = \frac{\lambda \tilde{z}}{N\Delta f} \quad (2.6.3, c)$$

We refer to these transforms as 1-D and 2-D **Discrete Kirchhoff-Rayleigh-Sommerfeld Transforms (DKRST)**. When  $\tilde{z} \rightarrow 0$ , DKRS-transform degenerates into the identical transform. When  $\tilde{z} \rightarrow \infty$ , DKRS-transform converts to discrete Fresnel transforms. In distinction from 2-D DFTs and DFrTs, 2-D Discrete KRS-transform is inseparable transform.

As one can see from Eqs. 2.6.3, Discrete Kirchhoff-Rayleigh-Sommerfeld transforms are digital convolutions. Therefore, they can be computed using FFT as:

$$\{\alpha_r\} = \text{IFFT}\left\{\text{FFT}\{[a_k]\} \bullet \text{FFT}[KRST_{\tilde{z},\mu}(\mathbf{n})]\right\}, \quad (2.6.4)$$

From this representation, inverse DKRS-transform can be obtained as:

$$\{\tilde{a}_k\} = \text{IFFT}\left\{\text{FFT}\{\alpha_r\} \bullet \frac{1}{\text{FFT}[KRST_{\tilde{z},\mu}(\mathbf{n})]}\right\}, \quad (2.6.5)$$

## Appendix

### A2. 1. Inverse scaled DFT

Scaled DFT

$$\alpha_r^\sigma = \frac{1}{\sqrt{\sigma N}} \sum_{k=0}^{N-1} a_k \exp\left(i2\pi \frac{kr}{\sigma N}\right) \quad (\text{A2.1.1})$$

has its inverse only if  $\sigma N$  is an integer number ( $\sigma N \in Z$ ). In this case, inverse ScDFT, for  $\sigma > 1$ , is defined as:

$$a_k^\sigma = \frac{1}{\sqrt{\sigma N}} \sum_{r=0}^{\sigma N-1} \alpha_r \exp\left(-i2\pi \frac{kr}{\sigma N}\right) = \begin{cases} a_k, & k = 0, 1, \dots, N-1 \\ 0, & k = N, N+1, \dots, \sigma N-1 \end{cases}$$

Proof:

$$\begin{aligned} a_k^\sigma &= \frac{1}{\sqrt{\sigma N}} \sum_{r=0}^{\sigma N-1} \alpha_r \exp\left(-i2\pi \frac{kr}{\sigma N}\right) = \frac{1}{\sigma N} \sum_{r=0}^{\sigma N-1} \left[ \sum_{n=0}^{N-1} a_n \exp\left(i2\pi \frac{nr}{\sigma N}\right) \right] \exp\left(-i2\pi \frac{kr}{\sigma N}\right) = \\ &= \frac{1}{\sigma N} \sum_{n=0}^{N-1} a_n \left[ \sum_{r=0}^{\sigma N-1} \exp\left(i2\pi \frac{n-k}{\sigma N} r\right) \right] = \frac{1}{\sigma N} \sum_{n=0}^{N-1} a_n \frac{\exp[i2\pi(n-k)] - 1}{\exp\left(i2\pi \frac{n-k}{\sigma N}\right) - 1} = \\ &= \frac{1}{\sigma N} \sum_{n=0}^{N-1} a_n \frac{\sin[\pi(n-k)]}{\sin\left(\pi \frac{n-k}{\sigma N}\right)} \exp\left[i\pi \frac{\sigma N-1}{\sigma N} (n-k)\right] = \begin{cases} a_n, & k = 0, 1, \dots, N-1 \\ 0, & k = N, N+1, \dots, \sigma N-1 \end{cases} \end{aligned} \quad (\text{A2.1.2})$$

as for  $k = N, N+1, \dots, \sigma N-1$ ,  $\sin[\pi(n-k)] = 0$  and  $\sin\left(\pi \frac{n-k}{\sigma N}\right) \neq 0$

## A2. 2. Approximation of function frined(.)

Consider a discrete analog of the known relationship ([9]):

$$\int_{-\infty}^{\infty} \exp(i\pi\sigma^2 x^2) \exp(-i2\pi fx) dx = \frac{\sqrt{i}}{\sigma} \exp\left(-i\pi \frac{f^2}{\sigma^2}\right) \quad (\text{A.2.2.1})$$

By definition of integral:

$$\int_{-\infty}^{\infty} \exp(i\pi\sigma^2 x^2) \exp(-i2\pi fx) dx = \lim_{\substack{N \rightarrow \infty \\ \Delta x \rightarrow 0}} \sum_{k=-N/2}^{N/2-1} \exp(i\pi\sigma^2 k^2 \Delta x^2) \exp(-i2\pi rk \Delta x \Delta f) \Delta x, \quad (\text{A.2.2.2})$$

where  $x = k\Delta x$ , and the integral is considered in points  $f = r\Delta f$ . Select  $\Delta f \Delta x = 1/N$  and assume that  $N$  is an odd number. Then

$$\int_{-\infty}^{\infty} \exp(i\pi\sigma^2 x^2) \exp(-i2\pi fx) dx = \lim_{\substack{N \rightarrow \infty \\ \Delta x \rightarrow 0}} \sum_{k=-(N-1)/2}^{(N-1)/2} \exp(i\pi\sigma^2 k^2 \Delta x^2) \exp(-i2\pi rk \Delta x \Delta f) \Delta x \quad (\text{A.2.2.3})$$

Therefore

$$\lim_{\substack{N \rightarrow \infty \\ \Delta x \rightarrow 0}} \frac{1}{N\Delta f} \sum_{k=-(N-1)/2}^{(N-1)/2} \exp\left(i\pi \frac{\sigma^2}{N\Delta f^2} \frac{k^2}{N^2}\right) \exp\left(-i2\pi \frac{rk}{N}\right) = \lim_{N \rightarrow \infty} \frac{\sqrt{i}}{\sigma} \exp\left(-i\pi \frac{r^2 \Delta f^2}{\sigma^2}\right). \quad (\text{A.2.2.4})$$

Denote:  $\sigma^2 / N\Delta f^2 = q$ . Then

$$\begin{aligned} \lim_{N \rightarrow \infty} \frac{1}{N\Delta f} \sum_{k=-(N-1)/2}^{(N-1)/2} \exp\left(i\pi \frac{qk^2}{N}\right) \exp\left(-i2\pi \frac{rk}{N}\right) &= \lim_{N \rightarrow \infty} \frac{\sqrt{i}}{\Delta f \sqrt{Nq}} \exp\left(-i\pi \frac{r^2 \Delta f^2}{q\Delta f^2 N}\right) \\ &= \lim_{N \rightarrow \infty} \frac{\sqrt{i}}{\Delta f \sqrt{Nq}} \exp\left(-i\pi \frac{r^2}{qN}\right), \end{aligned} \quad (\text{A.2.2.5})$$

or

$$\lim_{N \rightarrow \infty} \frac{1}{N} \sum_{k=-(N-1)/2}^{(N-1)/2} \exp\left(i\pi \frac{qk^2}{N}\right) \exp\left(-i2\pi \frac{rk}{N}\right) = \lim_{N \rightarrow \infty} \frac{\sqrt{i}}{\sqrt{Nq}} \exp\left(-i\pi \frac{r^2}{qN}\right). \quad (\text{A.2.2.6})$$

Therefore, one can say that

$$\frac{1}{N} \sum_{k=-(N-1)/2}^{(N-1)/2} \exp\left(i\pi \frac{qk^2}{N}\right) \exp\left(-i2\pi \frac{rk}{N}\right) \cong \frac{\sqrt{i}}{\sqrt{Nq}} \exp\left(-i\pi \frac{r^2}{qN}\right). \quad (\text{A.2.2.7})$$

It is assumed in this formula that both  $k$  and  $r$  are running in the range  $-(N-1)/2, \dots, 0, \dots, (N-1)/2$ . Introduce variables  $n = k + (N-1)/2$  and  $s = r + (N-1)/2$  to convert this formula to the formula that corresponds to the canonical DFT in which variables  $n$  and  $s$  run in the range  $0, \dots, N-1$ .

$$\begin{aligned}
& \frac{1}{N} \sum_{k=-(N-1)/2}^{(N-1)/2} \exp\left(i\pi \frac{qk^2}{N}\right) \exp\left(-i2\pi \frac{rk}{N}\right) = \\
& \frac{1}{N} \sum_{n=0}^{N-1} \exp\left\{i\pi \frac{q[n-(N-1)/2]^2}{N}\right\} \exp\left\{-i2\pi \frac{[s-(N-1)/2][n-(N-1)/2]}{N}\right\} = \\
& \frac{1}{N} \exp\left[i\pi \left(\frac{q}{2}-1\right) \frac{(N-1)^2}{2N}\right] \exp\left[i\pi \frac{s(N-1)}{N}\right] \times \\
& \sum_{n=0}^{N-1} \exp\left(i\pi \frac{qn^2}{N}\right) \exp\left[i\pi \frac{(1-q)(N-1)}{N} n\right] \exp\left(-i2\pi \frac{ns}{N}\right) \cong \\
& \frac{\sqrt{i}}{\sqrt{Nq}} \exp\left\{-i\pi \frac{[s-(N-1)/2]^2}{qN}\right\}. \tag{A.2.2.8}
\end{aligned}$$

From this we have:

$$\begin{aligned}
& \frac{1}{N} \sum_{n=0}^{N-1} \exp\left(i\pi \frac{qn^2}{N}\right) \exp\left(-i2\pi \frac{n[s-(1-q)(N-1)/2]}{N}\right) \cong \\
& \frac{\sqrt{i}}{\sqrt{Nq}} \exp\left\{-i\pi \left[\left(\frac{q}{2}-1\right) \frac{(N-1)^2}{2N}\right]\right\} \exp\left[-i\pi \frac{s(N-1)}{N}\right] \exp\left\{-i\pi \frac{[s-(N-1)/2]^2}{qN}\right\} \\
& \tag{A.2.2.9}
\end{aligned}$$

within boundaries  $(1-q)\frac{N-1}{2} < s < (1+q)\frac{N-1}{2}$ ;  $0 \leq q \leq 1$ , or finally

$$\begin{aligned}
& \frac{1}{N} \sum_{n=0}^{N-1} \exp\left(i\pi \frac{qn^2}{N}\right) \exp\left[-i2\pi \frac{n(s-v_q)}{N}\right] \cong \sqrt{\frac{i}{Nq}} \exp\left[-i\pi \frac{(s-v_q)^2}{qN}\right] \text{rect}\left[\frac{s-v_q}{q(N-1)}\right], \\
& \tag{A.2.2.10}
\end{aligned}$$

where  $v_q = (1-q)(N-1)/2$ ,  $0 \leq q \leq 1$  and  $s$  runs from  $0$  to  $N-1$ .

Numerical evaluation of the relationship

$$\begin{aligned}
& \mathbf{RCT}(N; q; s) = \frac{1}{N} \sum_{n=0}^{N-1} \exp\left(i\pi \frac{qn^2}{N}\right) \exp\left[-i2\pi \frac{n(s-v_q)}{N}\right] / \sqrt{\frac{i}{Nq}} \exp\left[-i\pi \frac{(s-v_q)^2}{qN}\right] = \\
& \frac{\sqrt{q} \exp\left[i\pi \frac{(s-v_q)^2}{qN}\right]}{\sqrt{iN}} \sum_{n=0}^{N-1} \exp\left(i\pi \frac{qn^2}{N}\right) \exp\left[-i2\pi \frac{n(s-v_q)}{N}\right] \cong \text{rect}\left[\frac{s-v_q}{q(N-1)}\right] \\
& \tag{A.2.2.11}
\end{aligned}$$

confirms the validity of this approximation ([16]). This is illustrated in Fig. 9 for  $N=512$  and four different values of  $q$  (0.25; 0.5; 0.75 and 1.0). Rect-function of Eq. A.2.1.11 is shown in bold line.

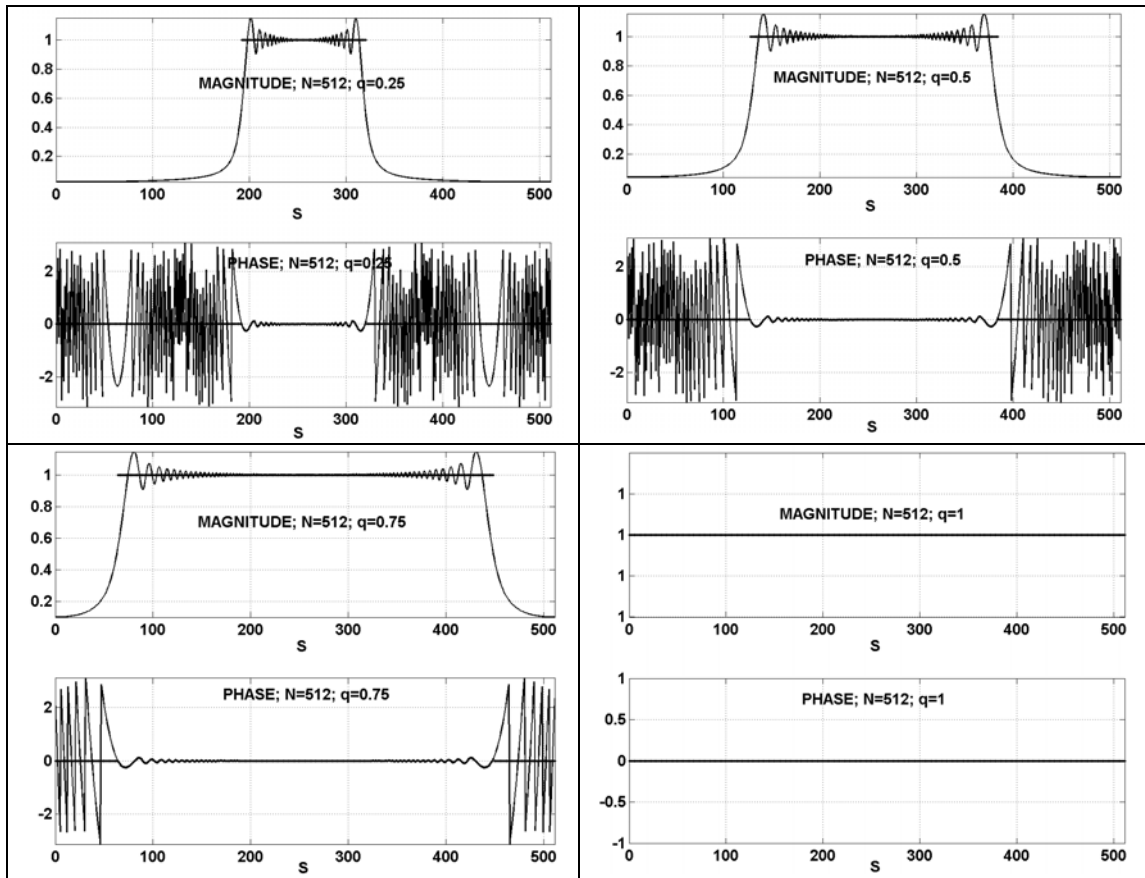


Fig. 9. Plots of absolute values (magnitude) and phase (in radians) of function  $RCT(N; q, s$ , Eq. 9.3.11, for  $N=512$  and four different values of  $q$  (0.25; 0.5; 0.75 and 1.0). Rect-function that approximates this function is shown in bold line.

### A2.3. Summary of the fast discrete diffraction transforms

Table.

Transform	
Canonical Discrete Fourier Transform (DFT)	$\alpha_r = \frac{1}{\sqrt{N}} \sum_{k=0}^{N-1} a_k \exp\left(i2\pi \frac{kr}{N}\right)$
Shifted DFT	$\alpha_r^{u,v} = \frac{1}{\sqrt{N}} \sum_{k=0}^{N-1} a_k \exp\left[i2\pi \frac{(k+u)(r+v)}{N}\right] = \frac{1}{\sqrt{N}} \sum_{k=0}^{N-1} a_k \exp\left(i2\pi \frac{\tilde{k}\tilde{r}}{N}\right)$
Discrete Cosine Transform (DCT)	$\alpha_r^{DCT} = \frac{2}{\sqrt{2N}} \sum_{k=0}^{N-1} a_k \cos\left(\pi \frac{k+1/2}{N} r\right)$
Discrete Cosine-Sine Transform (DcST)	$\alpha_r^{DcST} = \frac{2}{\sqrt{2N}} \sum_{k=0}^{N-1} a_k \sin\left(\pi \frac{k+1/2}{N} r\right)$
Scaled DFT	$\alpha_r^\sigma = \frac{1}{\sqrt{\sigma N}} \sum_{k=0}^{N-1} a_k \exp\left[i2\pi \frac{(k+u)(r+v)}{\sigma N}\right] = \frac{1}{\sqrt{\sigma N}} \sum_{k=0}^{N-1} a_k \exp\left(i2\pi \frac{\tilde{k}\tilde{r}}{\sigma N}\right)$
Scaled DFT as a cyclic convolution	$\alpha_r^\sigma = \frac{\exp\left(i\pi \frac{\tilde{r}^2}{\sigma N}\right)}{\sqrt{\sigma N}} \sum_{k=0}^{N-1} \left[ a_k \exp\left(i\pi \frac{\tilde{k}^2}{\sigma N}\right) \right] \exp\left[-i\pi \frac{(\tilde{k}-\tilde{r})^2}{\sigma N}\right]$
Canonical 2-D DFT	$\alpha_{r,s} = \frac{1}{\sqrt{N_1 N_2}} \sum_{k=0}^{N_1-1} \sum_{l=0}^{N_2-1} a_{k,l} \exp\left[i2\pi \left(\frac{kr}{N_1} + \frac{ls}{N_1}\right)\right]$
Affine DFT	$\alpha_{r,s} = \sum_{k=0}^{N_1-1} \sum_{l=0}^{N_2-1} a_{k,l} \exp\left[i2\pi \left(\frac{rk}{\sigma_A N_1} + \frac{sk}{\sigma_C N_1} + \frac{rl}{\sigma_B N_2} + \frac{sl}{\sigma_D N_2}\right)\right]$
Rotated DFT (RotDFT)	$\alpha_{r,s} = \sum_{k=0}^{N-1} \sum_{l=0}^{N-1} a_{k,l} \exp\left[i2\pi \left(\frac{r \cos \theta - s \sin \theta}{N} k + \frac{r \sin \theta + s \cos \theta}{N} l\right)\right] = \sum_{k=0}^{N-1} \sum_{l=0}^{N-1} a_{k,l} \exp\left[i2\pi \left(\frac{rk + sl}{N} \cos \theta - \frac{sk - rl}{N} \sin \theta\right)\right]$
Rotated Scaled DFT	$\alpha_{r,s} = \sum_{k=0}^{N-1} \sum_{l=0}^{N-1} a_{k,l} \exp\left[i2\pi \left(\frac{r \cos \theta - s \sin \theta}{\sigma N} k + \frac{r \sin \theta + s \cos \theta}{\sigma N} l\right)\right] = \sum_{k=0}^{N-1} \sum_{l=0}^{N-1} a_{k,l} \exp\left[i2\pi \left(\frac{rk + sl}{\sigma N} \cos \theta - \frac{sk - rl}{\sigma N} \sin \theta\right)\right]$
Discrete Sinc-function	$\text{sincd}(N, x) = \frac{\sin x}{N \sin(x/N)}$

Table(Ctnd.).

Transform	
Canonical Discrete Fresnel Transform (DFrT)	$\alpha_r = \frac{1}{\sqrt{N}} \sum_{k=0}^{N-1} a_k \exp \left[ i\pi \frac{(k/\mu - r\mu)^2}{N} \right]; \quad \mu^2 = \lambda Z / N \Delta f^2$
Shifted DFrT	$\alpha_r^{(\mu,w)} = \frac{1}{\sqrt{N}} \sum_{k=0}^{N-1} a_k \exp \left[ -i\pi \frac{(k\mu - r/\mu + w)^2}{N} \right]; \quad w = u/\mu - v\mu$
Fourier Reconstruction algorithm for Fresnel holograms	$\alpha_r^{(\mu,w)} = \frac{\exp \left( -i\pi \frac{r^2}{\mu^2 N} \right)}{\sqrt{N}} \sum_{k=0}^{N-1} a_k \exp \left[ -i\pi \frac{(k\mu + w)^2}{N} \right] \exp \left( i2\pi \frac{k + w/\mu}{N} r \right)$
Focal Plane invariant DFrT	$\alpha_r^{\left( \mu, \frac{N}{2\mu} \right)} = \frac{1}{\sqrt{N}} \sum_{k=0}^{N-1} a_k \exp \left\{ -i\pi \frac{[k\mu - (r - N/2)/\mu]^2}{N} \right\}$
Partial DFrT (PDFrT)	$\tilde{\alpha}_r^{(\mu,w)} = \frac{1}{\sqrt{N}} \sum_{k=0}^{N-1} a_k \exp \left( -i\pi \frac{k^2 \mu^2}{N} \right) \exp \left[ i2\pi \frac{k(r - w\mu)}{N} \right]$
Convolutional Discrete Fresnel Transform (ConvDFrT)	$\alpha_r = \sum_{k=0}^{N-1} a_k \text{frincd}(N; \mu^2; r + w - k) = \frac{1}{N} \sum_{s=0}^{N-1} \left[ \sum_{k=0}^{N-1} a_k \exp \left( i2\pi \frac{k - r - w}{N} s \right) \right] \exp \left( -i\pi \frac{\mu^2 s^2}{N} \right)$
Convolutional reconstruction algorithm for Fresnel holograms	$\alpha_r = \frac{1}{N} \sum_{s=0}^{N-1} \left[ \sum_{k=0}^{N-1} a_k \exp \left( i2\pi \frac{ks}{N} \right) \right] \exp \left( -i\pi \frac{\mu^2 s^2}{N} \right) \exp \left( -i2\pi \frac{r + w}{N} s \right)$
Frincd-function	$\text{frincd}(N; q; x) = \frac{1}{N} \sum_{r=0}^{N-1} \exp \left( i\pi \frac{qr^2}{N} \right) \exp \left( -i2\pi \frac{xr}{N} \right)$ $\text{frincd}(N; 1; x) = \sqrt{\frac{i}{N}} \exp \left( -i\pi \frac{x^2}{N} \right); \quad x \in \mathcal{Z}$ <p>Analytical approximation:</p> $\text{frincd}(N; \pm q; x) \cong \sqrt{\frac{\pm i}{Nq}} \exp \left[ \mp i\pi \frac{x^2}{qN} \right] \text{rect} \left[ \frac{x}{q(N-1)} \right]$
Discrete Kirchhoff-Rayleigh-Sommerfeld Transform (DKRST)	$\alpha_r = \sum_{k=0}^{N-1} a_k \frac{\exp \left[ i2\pi \frac{\tilde{z}^2 \sqrt{1 + (\tilde{k} - \tilde{r})^2 / \tilde{z}^2}}{\mu^2 N} \right]}{1 + (\tilde{k} - \tilde{r})^2 / \tilde{z}^2}$

## References

1. J. Goodman, Introduction to Fourier Optics, McGraw-Hill, N.Y., 1996
2. L. Yaroslavsky, Digital Holography and Digital Image Processing, Kluwer Academic Publishers, Boston, 2004
3. L. Yaroslavsky, Shifted Discrete Fourier Transforms, in *Digital Signal Processing*, edited by V. Cappellini, Academic Press, London, 1980, p.69-74
4. L. R. Rabiner, R. W. Schafer, C. M. Rader, The chirp z-transform algorithm and its application, Bell System Tech. J., 1969, Vol. 48: 1249-1292
5. Xuegong Deng, Bipin Bihari, Jianhua Gan, Feng Zhao, and Ray T. Chen, Fast algorithms for chirp transforms with zooming-in ability and its application, J. Opt. Soc. Am. A, Vol. 17, No. 4, April 2000
6. V. Namias, The Fractional Order Fourier Transform and its Applications to quantum mechanics, J. Inst. Math. Appl. v. 25, 241-265 (1980)
7. D. H. Bailey, P. N. Swartztrauber, The Fractional Fourier Transform and applications, SIAM Rev. 1991, Vol. 33, 389-404
8. L. Yaroslavsky and N. Ben David, Focal plane invariant algorithm for digital reconstruction of holograms recorded in the near diffraction zone, In: Optical Measurement Systems for Industrial Inspection III, SPIE's Int. Symposium on Optical Metrology, 23-25 June 2003, Munich, Germany, W. Osten, K. Creath, M. Kujawinska, Eds., SPIE v. 5144, pp. 142-149
9. G. Pedrini, H. J. Tiziani, "Short-Coherence Digital Microscopy by Use of a Lensless Holographic Imaging System", Applied Optics-OT, 41, (22), 4489-4496, (2002).
10. E. Ciche, P. Marquet, Chr. Depeursinge, "Spatial filtering of zero-order and twin-image elimination in digital off-axis holography, Appl. Optics, v. 30, No. 23, Aug. 2000
11. I. S. Gradshteyn, I. M. Ryzhik, "Tables of integrals, series, and products", Academic Press, 1994.